Sowakiewicz, M., Blumenberg, M., Wicaw, D., Röhling, H. G., Scheeder, G., Hindenberg, K., ... Gerling, J. P. (2018). Zechstein Main Dolomite oil characteristics in the Southern Permian Basin: I. Polish and German sectors. *Marine and Petroleum Geology*, *93*, 356-375. https://doi.org/10.1016/j.marpetgeo.2018.03.023

Zechstein Main Dolomite oil characteristics in the Southern Permian Basin: I. Polish and German sectors

Mirosław Słowakiewicz[1,2,3], Martin Blumenberg[4], Dariusz Więcław[5], Heinz-Gerd Röhling[6], Georg Scheeder[4], Katja Hindenberg[7], Andrzej Leśniak[5], Erdem F. Idiz[8], Maurice E. Tucker[9], Richard D. Pancost[1,3], Maciej J. Kotarba[5], Johannes P. Gerling[4]

[1]Faculty of Geology, University of Warsaw, ul. Żwirki i Wigury 93, 02-089 Warszawa, Poland

[2]Organic Geochemistry Unit, School of Chemistry, University of Bristol, Cantock's Close, Bristol, BS8 1TS, UK; e-mail: m.slowakiewicz@gmail.com

[3]Cabot Institute, University of Bristol, Cantock's Close, Bristol, BS8 1UJ, UK

[4]Federal Institute for Geosciences and Natural Resources (BGR), Stilleweg 2, 30655 Hannover, Germany

[5]AGH University of Science and Technology, Faculty of Geology, Geophysics and Environmental Protection, Al. Mickiewicza 30, 30-059 Kraków, Poland

[6]State Authority for Mining, Energy and Geology, Geological Survey of Lower Saxony, Stilleweg 2, 30655 Hannover, Germany

[7]Institute of Bio- and Geosciences (IBG-3), Forschungszentrum Jülich GmbH, 52425 Jülich, Germany

[8]Department of Earth Sciences, University of Oxford, South Parks Road, Oxford, OX1 3AN, UK

[9]School of Earth Sciences, University of Bristol, BS8 1RJ, UK

Highlights

Main Dolomite oils from Germany and Poland constitute ten distinct groups

Aromatic C_{40} carotenoids are important correlative biomarker tools

Main Dolomite oils were generated from algal-rich marly carbonate/evaporite source rocks

Abstract

Geochemical analyses were used to classify 39 Zechstein (Late Permian, Lopingian) Main Dolomite (Ca2) crude oil samples from fields in the eastern and southern sector of the

Southern Permian Basin (SPB) of Europe and to provide new insights into the origin of the oil. Geochemical data indicate that Ca2 oils were generated in the early-to-late oil window and are mostly non-waxy oils. Various biomarker and stable carbon isotopic ratios were used to identify source and depositional settings for source rocks of Ca2 oils arranged within 10 distinct oil groups. Specifically, the geochemical analyses and oil-oil correlations revealed a set of characteristic biomarkers including an even-over-odd predominance (EOP) for the C_{20-30} *n*-alkanes, C_{40} carotenoid occurrence (isorenieratane, chlorobactane, *β*-isorenieratane), bisnorhopane/hopane (BNH/H) ratios >0.1, high abundances of C_{35} homohopanes and elevated concentrations of C_{32} and C_{34} homohopanes, a predominance of C_{29} homologues among 4-desmethyl steranes in the majority of oil samples, and a high abundance of diasteranes. Stable carbon isotopes and biomarkers provided ample evidence that Ca2 oils were generated from predominantly algal-rich marly carbonate/evaporite source rocks located in the lower slope/shallow-basin and lagoonal facies of the Ca2 basin, all deposited under suboxic-anoxic (euxinic) conditions. In the case of all higher maturity oils, the source rocks could not be reliably identified but high (>2) $C_{24}Tet/C_{23}$ values suggest a carbonate-evaporite depositional setting.

1. Introduction

The intracontinental Southern Permian Basin (SPB, Fig. 1) is the southern sub-basin of the Central European Basin (CEB) and one of the richest and most extensively studied petroliferous basins in Europe. It is Europe's largest sedimentary basin, evolving from the latest Carboniferous to Recent times (van Wees et al., 2000; Pharaoh et al., 2010), and extending over ~1,700 km from eastern England to the Belarussian-Polish and Polish-Lithuanian borders, and from Denmark to southern Germany, covering an area of ~ 700,000 km^2, in Zechstein Limestone [Ca1] time. The SPB oil is predominantly reservoired in porous and fractured carbonate facies of the Zechstein Main Dolomite (Ca2; also called the Staβfurt Karbonat in Germany) and it is believed to have been derived from Ca2 basin, slope and lagoon facies.

During Late Permian (Zechstein) greenhouse time, the SPB was repeatedly subjected to marine transgressions and regressions which resulted in the succession having a cyclic character of carbonate and evaporite deposits. Of these the second carbonate cycle (Ca2; Fig. 2) is economically the most important. Since the discovery of the Volkenroda field in 1930 in

Germany (Albrecht, 1932), about 258 additional fields have been discovered, including two large Ca2 fields in Poland: Barnówko-Mostno-Buszewo (1992; ~94 Mbo), and Lubiatów-Międzychód-Grotów (2001-2003; ~48 Mbo) (Doornenbal and Stevenson, 2010). The underlying and overlying evaporite rocks enclose the Ca2 (Kovalevych et al., 2008) and create an effective seal for hydrocarbons trapped in the Ca2 reservoir.

Although the Ca2 gas accumulations and their origin are relatively well understood (Krooss et al., 1995, 2005, 2006; Mingram et al., 2005; Jurisch and Krooss, 2008; Zdanowski and Wozniak, 2010; Kotarba et al., 2017), there are still many uncertainties concerning Ca2 oil-oil correlations and correlations of Ca2 oils to potential source rocks (Hofmann and Leythaeuser, 1995; Gerling et al., 1996a; Czechowski and Piela, 1997; Wehner, 1997; Czechowski et al., 1998; Kotarba et al., 1998, 2000; Hindenberg, 1999; Grelowski and Czechowski, 2010; Mikołajewski et al., 2012; Hammes et al., 2014; Petersen et al., 2016). Furthermore, the lack of sufficient information prevents the establishment of oil families, an understanding of their origin, the prediction of migration routes and possible secondary processes.

In this paper, we integrate the available and newly-generated molecular and isotopic compositions of the Ca2 oils and identify their characteristic biomarkers. We evaluate the occurrence of the aromatic C_{40} carotenoids (i.e., chlorobactane, isorenieratane) which can be used to infer water column stratification and photic zone euxinia (PZE, Summons and Powell, 1986; Sinninghe Damsté et al., 1993). Our conclusions are integrated with other biomarker signatures to interpret past redox conditions and organic matter (OM) source, using stable carbon isotopes of saturated and aromatic fractions as well as distributions of *n*-alkanes, isoprenoids, tricyclic terpanes, hopanes and steranes. These data and interpretations are complemented by the conclusions on the origin of Ca2 oils derived from the pioneering work of Gerling et al. (1996a), subsequently continued by others (e.g., Czechowski et al., 1998; Kotarba et al., 1998, 2000, 2003; Hindenberg, 1999; Kotarba and Wagner, 2007; Grelowski and Czechowski, 2010; Słowakiewicz and Gąsiewicz, 2013).

2. Geological setting

In the Permian, the CEB mainly consisted of two WNW – ESE striking basins, called the Northern and Southern Permian basins (NPB and SPB). During sedimentation of the

Zechstein Group, which represents approximately ~2 to 2.6 m.y. (Changhsingian; Szurlies, 2013; Hounslow and Balabanov *in press*), the SPB was located in northern Pangea at palaeolatitudes of 10-15°N. It was separated from the NPB by a chain of palaeo-highs, i.e., the Mid North Sea High and Ringkøbing-Fyn High (Fig. 1), both of which were covered by sediments during the latest Zechstein (Hiete et al., 2005). The NPB and the SPB were both occupied by waters of the epicontinental Zechstein Sea. Marine ingression from the Boreal Sea and the Palaeo-Tethys into the mainly restricted basins resulted in deposition of a thick, cyclic succession (as much as ~2 km) of bedded carbonate, sulphate and halite with minor potash salt and with relatively thin intercalations of clastic sediments (Richter-Bernburg, 1953; Taylor, 1998; Paul, 2010). Four major carbonate-evaporite cycles (Z1-Z4) are recognised across the SPB, overlain by three thinner clastic-evaporite cycles (Z5-Z7), reflecting a more regressive trend in the upper part with an increase of fluvial deposits delivered from surrounding highlands to the basin centre. Only in the central parts of the North German sub-Basin (NGB) do the upper three cycles contain halite (Best, 1989). Many sulphate evaporites of the Zechstein Group resemble those of the modern Abu Dhabi and Qatar sabkhas, whereas the configuration of the basin and its seawater circulation may have resembled that of the present-day Mediterranean Sea.

3. Potential source rock settings within the Ca2 strata

Previously invoked concepts for potential source rocks of Ca2 oils have evolved over the past 20 years, from models invoking lower slope-basinal facies (Karnin et al., 1996; Kotarba et al., 2003) to inner platform-slope-lagoonal facies (Pletsch et al., 2010) to lagoonal and lower slope-shallow basin facies containing mixed algal-microbial-terrigenous types of OM with relatively low total organic carbon (TOC) content (Gerling et al., 1996a; Schwark et al., 1998; Hindenberg, 1999; Kotarba and Wagner, 2007; Słowakiewicz and Mikołajewski, 2011; Słowakiewicz and Gąsiewicz, 2013; Słowakiewicz et al., 2013, 2015, 2016a; Kosakowski and Krajewski, 2014, 2015). Recently, biomarker studies have helped to characterise the palaeoenvironmental and palaeoceanographic conditions during the deposition of Ca2 facies (Słowakiewicz et al., 2015, 2016a), and suggested characteristic biomarkers and biomarker ratios for the individual facies types (Słowakiewicz, 2016).

As previously postulated (e.g., Gerling et al., 1996b; Karnin et al., 1996; Czechowski et al., 1998; Kotarba et al., 1998, 2000, 2003; Hindenberg, 1999; Kotarba and Wagner, 2007;

126 Słowakiewicz and Gąsiewicz, 2013), the Ca2 intraformationally generated oil, which
127 migrated to fill pores, fissures, fractures and karst cavities (Słowakiewicz et al., 2016b); this
128 resulted in an artificially-enhanced enrichment in OM volumes for the Ca2 sequence as a
129 whole. This process is evident in the elevated Rock-Eval production index (PI) values
130 (PI>0.4), which were interpreted by Kotarba et al. (2003) as implying that >30% of their
131 overall Ca2 rock sample population was impregnated by migrated hydrocarbons.

132 ## 4. Materials and Methods

133 *4.1. Sample collection*

134 Thirty-nine crude oil samples were collected from 1) NW Poland (Kamień Pomorski and
135 Pomerania carbonate platforms) and SW Poland (west Fore-Sudetic Monocline), which were
136 situated on the northern and southern margins of the SPB, respectively (Fig. 2a,b); 2) NE
137 Germany (Mecklenburg-Vorpommern) and SE Germany (Brandenburg), which were parts of
138 the NGB situated on the northern and southern margins of the SPB (Fig. 2a,b); and 3) the
139 northern part of the Thuringian (sub)-Basin (TB, Germany), which was located on the south-
140 central margin of the SPB (Fig. 2c). Two crude oils (PL-4 and -5) are reservoired in
141 Zechstein Platy Dolomite (Ca3) facies but due to the geochemical similarity to the Ca2 oils
142 they are included in our overall dataset.

143 *4.2. Extraction and biomarker analyses*

144 About 5 - 100 mg of the stabilized crude oil samples were subjected to a fractionation
145 procedure. Prior to this, asphaltenes were precipitated over 12 h by adding 2 mL
146 dichloromethane (DCM) and 60 mL petroleum ether to (at maximum) 100 mg of sample.
147 Subsequently, the mixtures were centrifuged at 3000 rpm for 15 min. The supernatant
148 solution containing maltenes was collected and the solvent removed through evaporation in a
149 nitrogen atmosphere at 35 °C. Parallel asphaltene precipitation of a sample of known
150 composition (Norwegian Geochemical Standard NSO-1 oil) for every sample sequence
151 assured reproducibility control of the method. The residual maltenes (up to 100 mg) were
152 separated into aliphatic and aromatic fractions as well as into hetero-compounds (NSO-
153 compounds) on silica gel (activated at 240 °C for 12 h) by mid-pressure liquid
154 chromatography (BESTA-Technik für Chromatographie GmbH), using a sequence of organic
155 solvents of different polarity (iso-hexane, iso-hexane/DCM (2:1; v:v), DCM/MeOH (2:1; v:v).

156 The distribution of compounds contained in the aliphatic and aromatic fractions was
157 determined with gas chromatography-mass spectrometry (GC-MS), using an Agilent-7890

158 instrument equipped with a PTV inlet splitting on two DB-1 columns (each 50 m; 0.2 mm
159 i.d.; film thickness 0.11 µm), one coupled to a flame ionisation detector (FID), the other one
160 to an Agilent 7000 QQQ mass spectrometer (in Germany); and an Agilent 7890A equipped
161 with a fused silica capillary column (60 m, 0.25 mm i.d.) coated with 95 % methyl-/5 %
162 phenylsiloxane phase (DB-5MS, film thickness 0.25 µm) and coupled with an Agilent 5975C
163 mass selective detector (in Poland). Helium was used as the carrier gas. The columns were
164 heated from 60 °C to 150 °C, at a rate of 20 °C min^{-1}, then heated to 320 °C, at a rate of
165 4.5 °C min^{-1} (held for 15 min). Measurements of aliphatic fractions were carried out using
166 parent-daughter-scans via multiple-reaction-monitoring (MRM). Aromatic fractions were
167 analysed in full-scan mode. Peak ratio calculations for GC-FID and GC-MS were done from
168 integrated area:area and the biomarker ratios were computed as area:area as well.
169 Isorenieratane was identified from co-elution experiments with an aliphatic fraction from the
170 Rhaetian Kössen Formation, Germany and the Changhsingian Main Dolomite, Poland (and
171 the presence of spectral characteristics typical for aryl isoprenoids; e.g. *m/z* 133; Grice et al.,
172 1996; Koopmans et al., 1996; Słowakiewicz et al., 2015). Quantification was achieved
173 through comparison of the FID trace of the isorenieratane peak of the sample with an *n*-C_{40}
174 alkane calibration sample set with known concentrations.

175

176 *4.3. Stable carbon isotope analyses*

177 Stable carbon isotope ratios of the C_{15+} saturated and aromatic hydrocarbon fractions
178 were determined after combustion (Schoell, 1984) using a Dual-Inlet VG-903 isotope mass
179 spectrometer. The $\delta^{13}C$ values are reported relative to the Vienna Pee Dee Belemnite (VPDB)
180 standard, and the analytical error, determined by using co-injected standards, is ±0.2‰.

181 **5. Results and discussion**

182 Several parameters were excluded from analysis because they are readily altered by
183 thermal maturity: API gravity, sulphur content, saturated/aromatic hydrocarbon ratio, and the
184 weight percent <C_{15} hydrocarbon fraction.

185

186 *5.1. Maturity*

187 The thermal maturity of oils (Table 1, 2) was evaluated based on analysis of the saturated
188 and aromatic hydrocarbons including ratios of pristane/*n*-heptadecane (Pr/*n*-C_{17}) and

phytane/*n*-octadecane (Ph/*n*-C_{18}), C_{27} 18α-trisnorneohopane (Ts) to C_{27} 17α-trisnorhopane (Tm) (Ts/(Tm), C_{27} diasteranes /(diasteranes + regular steranes) vs Ts/Tm (controlled by thermal maturity and source, Moldowan et al., 1994), C_{30} moretane/C_{30} hopane (M/H), 20S/(20S+20R) for αααC_{29} steranes, ββ/(αα + ββ) for αββC_{29} steranes, triaromatic steroids (TA[I]/TA[I+II]), 4- to 1-methyldibenzothiophene (MDR), and the calculated vitrinite reflectance (Rm = 0.073 x MDR + 0.51, Radke, 1988). Using a variety of maturity parameters can help to overcome possible fractionation effects resulting from adsorption of OM on mineral surfaces, the expulsion process, and subsequent migration of oil (Zhusheng et al., 1988), all of which may affect maturation signatures and variations in biomarker distributions.

The isoprenoid-based ratios Pr/*n*-C_{17} and Ph/*n*-C_{18} show values of 0.07 – 1.17 and 0.2 – 1.5, respectively (Table 1, Fig. 3). As a result of the preferential release of *n*-alkanes during maturation, these ratios decrease with increasing thermal stress, but they also can be affected by organofacies variation and biodegradation (Peters et al., 2005). These ratios are the lowest, respectively, in BGR-13 and PL-6 and the highest in PL-5 (Table 1). The Pr/*n*-C_{17} ratio shows groupings of Ca2 oils (Fig. 3) most likely resulting from different thermal maturity of OM.

The Ts/Tm ratios range from 0.6 – 11.8 and are the highest (>4) in BGR-9, PL-12, -18 and -19, and this ratio appears to have been maturity-controlled in the Ca2 oil samples (Fig. 4a). However, it can also be affected by lithology: in carbonate settings Tm is preferentially generated (Peters et al., 2005). The moretane/hopane (M/H) ratios vary between 0.05 and 0.19 in all samples (Table 2). The M/H ratios could not be determined in BGR-9, PL-18, -19, and -24 due to the presence of only trace amounts of these biomarkers.

The isomerisation equilibrium for ββ/(αα + ββ) and 20S/(20S+20R) C_{29} steranes lies between 0.67 – 0.71 and 0.52 – 0.57, respectively (Seifert and Moldowan, 1986). Both parameters are valid through peak oil generation. In our samples, values for the ββ/(αα + ββ) ratio vary between 0.52 and 0.62, whereas the 20S/(20S+20R) values range from 0.43 to 0.56, indicating generation from the early oil phase to peak oil window (Table 2). Huang et al. (1990) noted that oils derived from gypsum, rock salt and carbonate -enriched source rocks show lower ββ/(αα + ββ) values than for 20S/(20S+20R). Hence, the ββ/(αα + ββ) C_{29} sterane ratio may not be reliable as a direct maturity indicator because it could be affected by source rock lithology. The TA(I)/TA(I+II) ratio (Mackenzie et al., 1981) increases with increasing

maturity (Beach et al., 1989) and is descriptive for mature and late mature stages of oil generation (Peters et al., 2005). Values for TA(I)/TA(I+II) ratio are between 0.04 and 1 indicating generation from the peak oil phase to late oil window (Table 2).

MDR values in the studied samples vary between 1.5 and 8.3 giving maturities in the range of 0.6%Rm to 1.1%Rm (Fig. 4b, Table 2), indicating early to peak/late oil window generation.

Collectively, our data indicate that the majority of oil samples were generated in the peak oil window, whereas seven oils located in SE NGB (BGR-6, -7, -8, -9), NW (PL-18, -19) and SW (PL-24) Poland were generated in the late oil window (Fig. 2, Table 2), which suggests a different thermal history. In addition, the maturity estimation for BGR-1 is inconclusive (high Rm, low sterane and triaromatic steroid ratios), but by comparison to other oils we suggest BGR-1 was also likely generated in the peak oil window.

Grelowski and Czechowski (2011) noted that crude oils reservoired in Ca2 facies in SW Poland (Gorzów Block located north of the Fore-Sudetic Monocline) have a higher maturity than Ca2 oils located in NW Poland. However, high maturity of PL-18 and -19 and to some extent PL-13 located in NW Poland suggests local high thermal maturity conditions. In the case of oils located in the TB, corresponding natural gases may indicate slightly higher maturities than in the other regions of Germany (Gerling et al., 1996a).

5.2. Palaeosetting during oil source rock deposition

5.2.1 Stable carbon isotopes of hydrocarbon fractions

$\delta^{13}C$ values of oils and oil fractions can be used for petroleum correlation (Peters et al., 2005), age classification (Andrusevich et al., 1998) or reconstruction of the depositional environment (Sofer, 1984; Chung et al., 1992). $\delta^{13}C$ values of the saturated fraction of the studied oils vary between -30.6 and -24.3‰, whereas the aromatic fraction has $\delta^{13}C$ values ranging from -31 to -23.9‰ (Fig. 5, Table 1). The canonical variable (CV=0.47; Sofer, 1984), which separates non-waxy (marine) and waxy (non-marine) oils, varies between -4.4 and 2.2. All signatures indicate that the source rocks for the studied oils were deposited in a marine setting. However, the BGR-4 oil falls slightly off the transition field between marine and terrigenous origin of oils, suggesting some contribution from terrigenous OM (CV = 2.2), but other biomarker signatures (e.g. homohopanes, steranes) strongly support predominantly marine OM.

Figure 5 shows several oil groupings (described in Section 6 in more detail); for example PL-4, -5, -12, -13 and -21 (NW Poland), occurring in Ca2 lower slope-shallow basin facies (Fig. 2), have the lowest $\delta^{13}C$ values. Higher $\delta^{13}C$ values are given by BGR-6, -7, -8 and -9, which make up another group of oils located in the TB and reservoired in lagoonal facies (Fig. 2). The highest $\delta^{13}C$ values (~-26 to -24 ‰) are in BGR-12, -13, -14, PL-6 and -7 located in SE Germany and SW Poland, respectively, and occurring in lagoonal and inner shoal facies. Other oil groups, like PL-16, -18, -19 and -20, or BGR-4, rather reflect individual oil-fields which may have been sourced from a different type of OM. Stable carbon isotope ratios must be used with caution in indicating source input because of fractionations during and after formation of the OM. Therefore, $\delta^{13}C$ isotopes should be used in tandem with other source- and age- diagnostic biomarkers which would allow more confident assessment of OM input (Peters et al., 2005). Nonetheless, Simoneit et al. (1993) also reported that $\delta^{13}C$ values of Permian marine OM range from -31 to -26 ‰, which are almost entirely within the range for saturated and aromatic fractions of Ca2 oils, suggesting predominantly a common source of marine OM. The heaviest $\delta^{13}C$ values in BGR-12, -13, -14, PL-6 and -7 suggest algal-rich OM that was probably deposited in a hypersaline environment (Table 1; Grice et al., 1998).

5.2.2 Water column stratification inferred from Ca2 oils

A suite of biomarkers was used to assess redox conditions and depositional environment during formation of source rocks for the investigated crude oils including the carbon preference index (CPI), Pr/*n*-C_{17} versus Ph/*n*-C_{18}, even-over-odd predominance (EOP) of *n*-alkanes, C_{31}-C_{35} homohopane distributions, the homohopane index (HHI) expressed as $C_{35}/(C_{31}$-$C_{35})$ and $C_{35}S/C_{34}S$, the concentration of isorenieratene and chlorobactene derivatives, 28,30-bisnorhopane (BNH) abundance expressed as BNH/C_{30} 17α-hopane (BNH/H), and gammacerane abundance expressed as gammacerane/C_{30} 17α-hopane (G/H) (Table 1).

The calculated CPI for almost all oils is close to 1.0 (Table 1) but an EOP for the C_{20-30} *n*-alkanes is observed in some oils (Fig. 6). An EOP is typical of biomass deposited in restricted marine carbonate/evaporite facies (Palacas et al., 1984; Mello et al., 1988a,b).

The patterns in the Pr/*n*-C_{17} versus Ph/*n*-C_{18} plot (Fig. 3; Table 1) indicate primary accumulation of marine OM under reducing conditions (Connan and Cassou, 1980; Palacas et al., 1988) for the source rocks of the Ca2 oils. However, these values can be thermally modified in oils of higher maturity (BGR-6, -7, -8, -9, PL-18, -19 and -24).

Homohopane distributions (Fig. 7) can be utilized to differentiate between oxic and reducing palaeodepositional environments, but the distributions can be affected by maturity and secondary alteration (Peters and Moldowan, 1991). The distribution for oils from NE Germany and NW Poland is characterised by elevated relative abundances of C_{35} homohopanes indicating that Zechstein carbonate and evaporite facies were deposited in a restricted setting with anoxic bottom water (Boon et al., 1983; Connan et al., 1986; Fu et al., 1986; ten Haven et al., 1988; Mello et al., 1988a,b; Clark and Philp, 1989; Słowakiewicz et al., 2015, 2016a); such conditions have been interpreted to be accompanied by the presence of reduced sulphur species in the water column (ten Haven et al., 1988; Sinninghe Damsté et al., 1995a). The reducing depositional conditions are also expressed by high HHIs (0.12-0.31, average 0.2) and $C_{35}S/C_{34}S$ (0.39-1.71) (Table 1). High HHIs in oil samples from NE Germany and NW Poland correspond well to high HHIs (0.12-0.56) reported predominantly from the Ca2 lower slope facies of the northeastern margin of the SPB (Słowakiewicz et al., 2016a). Oils from SE Germany and SW Poland have lower HHIs (0.12-0.18) and $C_{35}S/C_{34}S$ (0.74-1.05) (Table 1) suggesting suboxic/anoxic conditions consistent with relatively low HHIs (0.03-0.17[4], average 0.04-0.09) found in lagoonal facies (Słowakiewicz et al., 2016a).

All oil samples are characterised by the dominance of C_{30} 17α-hopane over lower or higher homologues in many oil samples (Fig. 6). The majority of oil samples have elevated abundances of C_{32} and C_{34} hopanes (particularly oils from S Germany, Fig. 6, 7), which are believed to indicate suboxic (high C_{32})/anoxic (high C_{34}) source-rock depositional environments (Peters and Moldowan, 1991). In addition, the dominance of 17α-C_{34} over C_{33} and C_{35} homologues indicates a carbonate lagoonal and evaporitic environment source (Waples and Machihara, 1991) or suggests an unknown source of bacteriohopanepolyols. BGR-9, PL-18, -19, -24 contain lower abundances or an absence of C_{31}-C_{35} homohopanes, likely due to thermal degradation during catagenesis (Table 1).

Biomarkers for anaerobic phototrophic green sulphur bacteria provide strong constraints on the redox state and water column stratification indicating PZE during source rock deposition (Summons and Powell, 1986; Sinninghe Damsté et al., 1993). Isorenieratane, *β*-isorenieratane, $C_{14\text{-}31}$ 2,3,6-aryl isoprenoids, and chlorobactane are present in most of the oils (Fig. 6, Table 1); they were not detected in BGR-13, PL-4, -5, -12, -13, -18, -19, -21, and -24. Concentrations of isorenieratane and chlorobactane vary between 16 and 710 µg g^{-1} oil and 1 and 65 µg g^{-1} oil, respectively. The overall highest concentrations of isorenieratene derivatives in our dataset occurred in oils from NE Germany and NW Poland (isorenieratane:

22-710 µg g^{-1} oil, chlorobactane: 3-65 µg g^{-1} oil, presence of *β*-isorenieratane; Fig. 6, Table 1).

Intriguingly, PL-12 and -21 oils, which do not contain isorenieratane and chlorobactane and were derived from the Ca2 lower slope facies, may mark the maximum basinward extent of PZE as it impinged on the NE slope of the SPB (Fig. 2a). Therefore, of all Ca2 oil biomarkers, the C_{40} carotenoids (isorenieratene derivatives) seem to be particularly important for Ca2 oils and source rocks. However, isorenieratene derivatives also occur in the Kimmeridge Clay Formation (e.g., van Kaam-Peters et al., 1988) and Oxford Clay Formation (Kenig et al., 2004), even though both are only regarded as source rocks for petroleum in the central and northern North Sea and are insignificant in the southern North Sea (Lott et al., 2010). They also occur in the Posidonia Shale Formation (Frimmel et al., 2004), important only in the Dutch rift basins and in Germany (Lott et al., 2010), in Devonian black shales (Joachimski et al., 2001) with no petroleum generation potential reported (Pletsch et al., 2010), Oligocene Menilite beds in the Polish and Ukrainian Carpathians (Kotarba et al., 2007) being the most important source rock for the Carpathian Province (Curtis et al., 2004, Kotarba and Koltun, 2006) and in Middle Rhaetian shales in Germany (Blumenberg et al., 2016). Consequently, French et al. (2015) concluded that in addition to PZE, other factors, such as an origin from microbial mats, an allochthonous input, planktonic origin or production of these biomarkers in 'no analogue' palaeoenvironments, should be taken into account to explain sources of isorenieratene derivatives.

Similarly, Słowakiewicz et al. (2015, 2016) only found isorenieratene derivatives in the shallow basin and lower slope facies and in lagoons of the northeastern and southern SPB. Reducing and even euxinic conditions likely existed in restricted lagoons dominated by production of microbialites under high salinity conditions, but isorenieratane and chlorobactane have not been detected in oolite shoal facies on the northeastern SPB, excluding redeposition of isorenieratene derivatives into subtidal settings of the Ca2 carbonate platform. However, the presence of isorenieratane and chlorobactane in lagoons and inner oolite shoals of the southern SPB suggests that such settings were their source in some Ca2 oils (i.e., BGR-12, -14, PL-10, -14, -16, -17, -20).

Anoxic conditions during deposition of source rocks are also confirmed by the occurrence of BNH detected in some oils (Table 1). BNH is a desmethylhopane of unknown origin but generally regarded as indicative of anoxic or euxinic deposition (e.g. Curiale et al., 1985;

Mello et al., 1990; Peters et al., 2005). The BNH/H ratio can be applied as a facies parameter, provided that the oil samples are not of too high maturity. BNH was detected in all oils from Poland (except for PL-3) and the BNH/H ratio in the Polish oils varies between 0.01 and 0.21. Abundant BNH in PL-18 and -19 indicates deposition of the source rock under clay-poor anoxic conditions (Katz and Elrod, 1983; Mello et al., 1988a; Curiale and Odermatt, 1989). Alternatively, the ratio may be affected by maturity as the relative amount of BNH can decline with increasing maturity (Peters et al., 2005). BNH (BNH/H 0.1 – 0.24) was also detected in the lowermost lower slope and shallow basin facies in the Ca2 on the northern margin of the eastern SPB (NW Poland, Słowakiewicz et al., 2015) which would suggest a common source for oils located in NW Poland. However, BNH was not detected in core samples from other parts of the SPB (Słowakiewicz et al., 2015). Nevertheless, its absence, also in oil samples from Germany and PL-3, does not preclude sedimentation under anoxic conditions.

Gammacerane, which is also present in the studied oils, is commonly invoked as additional evidence for a stratified water column in marine and non-marine depositional environments and/or specifically for hypersalinity (Moldowan et al., 1985; Jiamo et al., 1986; Sinninghe Damsté et al., 1995b). Gammacerane is believed to derive from tetrahymanol, which is produced by ciliates feeding on bacteria at oxic-anoxic transition zones. The abundance of gammacerane, expressed as G/H ratios (Sinninghe Damsté et al., 1995b), varies from 0.09 to 0.41 (Table 1). This may indicate slightly elevated salinity conditions during source rock deposition and corresponds to G/H (0.1-0.6) obtained from lower slope-shallow-basin and hypersaline lagoonal Ca2 facies (Słowakiewicz et al., 2015, 2016a). Gammacerane was not detected in BGR-9, PL-18 and -19.

In summary, our data suggest that Ca2 oils were generated from source rocks deposited under suboxic-anoxic(euxinic) marine carbonate-evaporite conditions with various strengths of water column stratification as evidenced by e.g., G/H. Gammacerane most commonly occurs in high abundance in the more restricted portions of the Ca2 basin and in restricted/hypersaline lagoons (Słowakiewicz et al., 2016a). Specifically, gammacerane abundance, which mirrors that of BNH, was detected in the lowermost sections of the lower slope facies and in the shallow-basin facies (NE margin of the Ca2 sea). It was interpreted as a record of marine hypersalinity during the early stage of the Ca2 transgression and carbonate precipitation as a part of the carbonate-evaporite cycle (Słowakiewicz et al., 2015), which additionally could support a carbonate-evaporite source for the Ca2 oils.

385 *5.3. Source of organic matter*

386 The tricyclic/17α-hopane ratio can be used for assessment of thermal maturity of oils
387 (Seifert and Moldowan, 1978), but it is commonly applied in the identification of the
388 principal source rocks (Peters et al., 2005). The tricyclic/17α-hopane ratio in the majority of
389 oil samples is 0.03-0.53 (average 0.16, standard deviation [SD] 0.14) and in two samples
390 (BGR-7 and -9) is >1 (Table 1). High (>1) tricyclic/17α-hopane ratios can be attributed to
391 marine depositional conditions rather than maturity (Seifert and Moldowan, 1979; Philp et al.,
392 1992). However, da Cruz et al. (2011) noted that oils with lower tricyclic/17α-hopane ratios,
393 usually interpreted as more mature oils, could be the consequence of anaerobic microbiota
394 degradation operating at higher temperatures. Regardless, a moderately high tricyclic/17α-
395 hopane ratio in tandem with high G/H and HHIs is consistent with deposition in a high-
396 salinity marine environment.

397 The source rock for Ca2 oils can also be explored using the C_{21}/C_{22} and C_{24}/C_{23} tricyclic
398 terpane ratios (in general, high C_{21}/C_{22} and low C_{24}/C_{23} occur in oils derived from carbonate
399 source rocks; Zumberge et al., 2005), the C_{19}/C_{21} tricyclic and C_{24} tetracyclic (Tet)/C_{23}
400 tricyclic terpane ratios (abundant C_{24} tetracyclic terpane in oils indicates carbonate or
401 evaporite source rocks, Palacas et al., 1984; Connan et al., 1986; Connan and Dessort, 1987;
402 Clark and Philp, 1989; or abundant tricyclic and tetracyclic terpanes can indicate high
403 thermal maturity, Farrimond et al., 1999), as well as the C_{29} 17α-norhopane/C_{30} 17α-hopane
404 ratio (C_{29}/H, high [>0.8] in oils derived from anoxic carbonate or marl source rocks; Palacas
405 et al., 1984; Clark and Philp, 1989).

406 For these oils, the C_{21}/C_{22} and C_{24}/C_{23} tricyclic terpane ratios suggest a marly carbonate-
407 evaporite depositional environment for Ca2 oils (Fig. 8). Similarly, the C_{19}/C_{21} tricyclic and
408 C_{24} Tet/C_{23} tricyclic terpane ratio indicates that Ca2 oil groups are facies-controlled rather
409 than maturity-controlled and high C_{24} Tet values imply a carbonate-evaporite depositional
410 environment for the source rocks (Fig. 9, Table 1). The C_{29}/H ratio, which ranges from 0.3 to
411 5.8, suggests terrigenous-carbonate/marl-type of OM, but the highest values (>2) could be
412 thermally controlled (Table 1).

413 The diasterane/sterane ratio expressed as C_{29} 13β,17α(H) (20S + 20R)/(C_{29}
414 5α,14α,17α(H) 20S + 20R + 5α,14β,17β(H) 20S + 20R) also helps to distinguish oils from
415 carbonate versus clastic source rocks (Mello et al., 1988a). High diasterane/sterane ratios are
416 typically interpreted to derive from clay-rich source rocks but high ratios have also been

observed in extracts from organic-lean and clay-poor carbonate rocks (Palacas et al., 1984; Moldowan et al., 1991), although high ratios in oils can also result from high thermal maturity or heavy biodegradation (Seifert and Moldowan, 1978, 1979). Van Kaam-Peters et al. (1998) observed that the diasterane/sterane ratio does not correlate with clay content but depends on the amount of clay relative to the amount of OM which can explain high diasterane/sterane ratios in oils derived from carbonate source rocks. The diasterane/sterane ratio in the majority of oil samples varies between 0.04 and 0.8 suggesting carbonate-evaporite source rocks with an abundant clay (marl) content (Table 1). The Pr/Ph versus C_{27} diasteranes /(diasteranes + regular steranes) plot also suggests a carbonate-evaporite depositional environment for the Ca2 oils' source rocks (Fig. 10). Very high diasterane/sterane ratios in PL-18, -19 and -24 (~2-3) can result from high thermal maturity (see Fig. 4 and Section 5.1, Seifert and Moldowan, 1978; van Graas, 1990), which is also confirmed by the reduced homohopane distributions, rendering the sterane data difficult to interpret in terms of OM source for those oils.

The dibenzothiophene/phenanthrene (DBT/P) ratio can also indicate source rock lithology, with carbonate rocks having ratios >1 and shales having ratios <1 (Hughes et al., 1995). In addition, high DBT/P ratios indicate the incorporation of reduced sulphur into OM in the source rocks, typical of carbonate-evaporite environments (Hughes et al., 1995). Accordingly, the source rock for oils in NE and SE Germany and BGR-9 contained relatively more clay/marl or evaporite (high C_{24}/C_{23} 0.65 – 0.99) (Fig. 8), than carbonate indications (C_{29}/H 0.37 – 0.68, DBT/P 0.09 – 1.18; Fig. 11; Table 1). In other oils the proportion of evaporite/clay decreases at the expense of marl/carbonate. However, Figure 11 and Table 1 show that the DBT/P ratio in PL-18 and -19 is very high (>13), which is likely thermally affected, and thus the obtained values cannot be reliably interpreted with respect to depositional setting. However, they can serve as reliable high-maturity indicators.

The Ca2 oils include abundant C_{27}-C_{29} 4-desmethyl steranes, with C_{29} steranes being more abundant than the total C_{27}-C_{28} steranes in 13 oil samples (Table 1, Fig. 12). The regular sterane distribution is consistent with either terrigenous or marine algal OM (Huang and Meinshein, 1979; Volkman, 1986; Volkman et al., 1998; Kodner et al., 2008), but is mostly indicative of algal-dominated carbonate marine settings (Palacas et al., 1984; Walter and Cassa, 1985; Grantham, 1986). The C_{27}/C_{29} and C_{28}/C_{29} sterane ratios in almost all samples vary from 0.3 to 1.7 and 0.3 to 0.9, respectively (Table 1). The highest of these sterane ratios are in PL-18 and -19 (Table 1, Fig. 12), and they are likely thermally controlled

and should be treated with caution. It also should be noted that a high-maturity interpretation for these samples is consistent with the high DBT/P and Ts/Tm versus C_{27} diasteranes/(diasteranes + regular steranes) ratios which also appear to be maturity-induced. In some cases, the C_{27}/C_{29} ratio can be used to indicate the relative inputs of algae relative to higher plants based on the dominance of C_{29} steroids in the latter (Huang and Meinschein, 1979); however, many algae also synthesize C_{29} sterols (Volkman, 1986; Volkman et al., 1998; Kodner et al., 2008). Although the C_{27}/C_{29} sterane ratio is typically >1 in marine-dominated depositional systems (Grantham and Wakefield, 1988), lower ratios are typical for predominantly marine Permian/Triassic sections (Cao et al., 2009; Hays et al., 2012; Słowakiewicz et al., 2015, 2016a).

The C_{28}/C_{29} sterane ratio has been used to distinguish Upper Cretaceous and Cenozoic oil from Palaeozoic or older oil (Grantham and Wakefield, 1988). These authors observed that the C_{28}/C_{29} sterane ratios for crude oils from marine source rocks with little or no terrigenous OM input are <0.5 for lower Palaeozoic and older oils, 0.4-0.7 for upper Palaeozoic to Lower Jurassic oils, and greater than approximately 0.7 for Upper Jurassic to Miocene oils. Earlier than the Mesozoic, however, C_{28} steranes were also likely derived from green algae, particularly prasinophytes (Kodner et al., 2008). It is also important to note that Słowakiewicz et al. (2016a) attributed the C_{28}/C_{29} sterane ratio variability to basin-scale differences in algal ecology. Therefore, we interpret the C_{28}/C_{29} sterane ratios (0.31 to 1.42, average ~0.47, excluding PL-18 and -19) as resulting from the proportion between C_{29} sterane-producing green algal groups and C_{28} sterane-producing red and prasinophyte algae (Kodner at al., 2008) in carbonate-evaporite environments. Thus, we conclude that the C_{28}/C_{29} sterane ratios in our sample set suggest significant input of green algae to the total biomass.

The regular steranes/17α-hopanes ratio is commonly used to reflect input of algae and higher plants versus bacteria, but increasing maturity elevates this ratio (Seifert and Moldowan, 1978; Requejo, 1994). The steranes/17α-hopanes ratio (0.1-2, Table 1) in our oil samples suggests a high proportion of algae to bacteria (average 0.55), yet some values in BGR-9, PL-18, -19 and -24 may result from high thermal maturity.

In summary, Ca2 oils were derived from a source rock whose OM contained various proportions of algae and bacteria and to a much lesser degree terrestrial plants depending on the type of the carbonate/evaporite depositional environment.

6. Implications for the inferred source of Ca2 oils and oil grouping

The Ca2 oil samples were derived from marine source rocks and the calculated CV (Table 1) classifies almost all Ca2 oils as non-waxy (CV<0.47). The biomarker parameters show that Ca2 oils were predominantly derived from mixed sulphate(+clay)-carbonate or marly carbonate lithofacies, i.e., the Ca2 source rocks as well as overlying and underlying anhydrites.

Collectively, the biomarker data presented here show the characteristic lipid biomarkers which can be applied in correlating Ca2 oils from shallow basin-lower slope and lagoonal-oolite shoal carbonate facies, located in the NE, SE and S SPB (Fig. 2). The marly carbonate source rocks are characterized by a significant contribution of sapropelic (algal + microbial) and subordinate clay(marl)-associated OM and they are chiefly located in lower slope/shallow-basin and lagoonal facies. The presence of clay minerals in the Ca2 carbonate matrix has also been noted by Schwark et al. (1998) and Grelowski and Czechowski (2011) and this is reflected by the increased abundance of diasteranes in the Ca2 oils. Generally, evaporite (anhydrite) rocks containing clays (e.g., chicken-wire anhydrite), but also marl and micritic limestone deposited under anoxic conditions, have long been considered as important source rocks for hydrocarbons (Kirkland and Evans, 1981; Sonnenfeld, 1985; Jiamo et al., 1986; Warren, 1986, 2011; Bousson, 1991; Edgell, 1991). The marginal and subaerial/shallow-water upper part of Z1 (Upper Anhydrite or Werra Anhydrite = Lower + Upper Anhydrite) and Z2 (Basal Anhydrite) anhydrite (Fig. 2) contains bituminous carbonate-anhydrite laminites and chicken-wire anhydrite (Taylor, 1998; Słowakiewicz and Mikołajewski, 2009; Peryt et al., 2010), which could have been an additional source for Ca2 oils. In addition, anhydrite is an important contributor to the Ca2 hypersaline lagoonal facies and interbeds with the Ca2 facies which would explain the evaporitic nature of the Ca2 oils studied and hence their additional sulphate-type OM source.

Ca2 oils share characteristic biomarker ratios which also are specific to particular SPB areas. Thus, they can be distinguished from oils generated from other source rocks and time intervals. The characteristic biomarkers of many Ca2 oils include: a) CPI ~1 and an EOP in the range of $C_{20\text{-}30}$ *n*-alkanes characteristic of carbonate/evaporite source rocks deposited in hypersaline settings; b) C_{40} carotenoids (isorenieratane (0)16-709 µg g^{-1} oil, chlorobactane (0)1-65 µg g^{-1} oil, *β*-isorenieratane), although these are only characteristic for oils reservoired

514 in (and most likely sourced from) shallow-basin to lower slope and lagoonal facies and are
515 characteristic of oils located in NE Germany and NW Poland; c) 28,30-bisnorhopane
516 (BNH/H 0.01-0.07) occurs in oils from the shallow-basin/lower slope-lagoonal facies in NW
517 and SW Poland; d) high abundance of C_{35} homohopanes was detected in oils from shallow-
518 basin/lower slope-lagoonal facies in NW Poland and NE Germany; e) a predominance of C_{34}
519 homohopanes over C_{33} and C_{35} homohopane homologues occurs in oils from lagoonal facies
520 in the TB; f) the majority of Ca2 oils have C_{29} steranes dominant over C_{27} and C_{28}
521 homologues but that is interpreted as deriving from a green algal marine, rather than
522 terrestrial, OM source; g) a high abundance of diasteranes relative to regular steranes (>0.1)
523 in almost all Ca2 oils is typical of petroleum derived from source rocks with an abundant clay
524 content; h) very high BNH/H (~0.2), Ts/Tm (>10), C_{29}/H (>4), DBT/P (>13) ratios are
525 characteristic of PL-18 and -19 suggesting relatively high thermal maturity and clay-poor
526 carbonate source rocks deposited under anoxic conditions. These suggested Ca2 characteristic
527 oil biomarkers correlate well with their analogues detected in Ca2 rock extracts
528 (Słowakiewicz, 2016), whereas the correlation for BGR-9, PL-18, -19 and -24 with potential
529 source rocks could not be reliably determined, probably due to elevated maturity levels.
530 Despite these general characteristics of Ca2 oils, based on $\delta^{13}C$ isotopes, homohopane
531 distributions, sterane ratios, isorenieratene derivatives, as well as regional occurrences and
532 previous interpretations on the local facies, the following oil sample classification is
533 suggested:

534 **Group 1**: BGR-12, -13, -14, PL-6 and 7 located in SE Germany and SW Poland and
535 reservoired in inner shoal (BGR-13, PL-6, -7) and lagoonal facies (BGR-12, -14). They are
536 characterised by the heaviest $\delta^{13}C$ isotopes (-24 to -26 ‰) and were derived from algal-rich
537 carbonate-evaporite source rocks deposited under anoxic (euxinic) conditions in Ca2
538 hypersaline lagoons. They are also characterised by slightly elevated C_{34} homohopanes
539 (except for BGR-14, Fig. 7).

540 **Group 2**: BGR-1, -2, -3 and -4 are reservoired in lower slope facies. $\delta^{13}C$ isotopes vary
541 between -27 and ~-25 ‰. The oils derived from predominantly algal (high sterane/17α-
542 hopane ratios) carbonate/evaporite Ca2 lower slope source rocks deposited under reducing
543 (HHI 0.19-0.23), euxinic (isorenieratane 159-408 µg g^{-1} oil, chlorobactane 27-65 µg g^{-1} oil)
544 and hypersaline conditions (G/H 0.16 to 0.19). They are characterised by abundant
545 concentrations of C_{35} homohopanes (Fig. 7).

Group 3: PL-1, -2, -3, -8, -9, -11, -15, -22, -23 are reservoired in lower slope and lagoonal/oolite shoal facies. $\delta^{13}C$ isotopes vary between ~-27 and~-26 ‰. Group 3 is similar to Group 2 oils but were derived from predominantly microbial-algal carbonate/evaporite Ca2 lower slope/lagoonal source rocks. Group 3 is characterised by the highest HHI (0.2-0.3), $C_{35}S/C_{34}S$ and G/H (0.2-0.35) ratios, and isorenieratane (23-709 µg g^{-1} oil) and chlorobactane ([0]3-53 µg g^{-1} oil) concentrations. They are also characterised by abundant C_{35} homohopanes (Fig. 7).

Group 4: BGR-5 (NE Germany) and BGR-10, -11 and -15 located in SE Germany are all reservoired in outer shoal facies. $\delta^{13}C$ isotopes vary between -26 and ~-28 ‰. The oils were derived from algal-rich (the highest sterane/17α-hopane ratios), carbonate/evaporite Ca2 lagoonal source rocks deposited under slightly reducing (HHI 0.12-0.16), euxinic (isorenieratane 125-360 µg g^{-1} oil, chlorobactane 17-47 µg g^{-1} oil) and hypersaline conditions (G/H 0.09-0.11). They are characterised by elevated C_{34} homohopanes (Fig. 7).

Group 5: Pl-16 and -20 located in SW Poland are reservoired in shallow-basin (PL-20) facies. This group is similar to Group 3 but has slightly elevated C_{34} homohopanes, abundant C_{27} steranes, lacks elevated C_{35} homohopanes (Fig. 7), and was deposited in reducing (HHI 0.17, BNH 0.06), euxinic (isorenieratane 46-50 µg g^{-1} oil) and hypersaline (G/H 0.23-0.27) conditions. Additionally, relatively low abundance of isorenieratene derivatives may suggest temporary euxinia and less restricted depositional conditions. PL-16 and -20 are derived from algal-rich carbonate/evaporite source rocks likely located in Ca2 shallow-basin facies.

Group 6: BGR-9 and PL-24 oils are reservoired in oolite (BGR-9) and shallow-marine dolo- and lime- mudstone (PL-24) facies. High thermal maturity evidenced by the high Ts/Tm (5.2-9.2, Table 2) and C_{29}/H (0.8-2) ratios, the low abundance of hopanes and absence of isorenieratane or chlorobactane precludes a reliable interpretation of the OM source for these oils. However, high $C_{24}Tet/C_{23}$ values might suggest a carbonate-evaporite depositional environment for the source rocks.

Group 7: PL-18 and -19 are reservoired in outer oolite facies of the Pomeranian carbonate platform (Fig. 2a). Thermal maturity is high (Table 2), similar to Group 6. High thermal maturity is supported by very high Ts/Tm (10.9-11.8, Table 2), diasterane/sterane (2.99-3.02), C_{29}/H (4.36-5.78), DBT/P (13.2-14.5, Fig. 9) and BNH/H (11-12) ratios. The C_{24}/C_{23} (0.78-0.85) tricyclic ratio and high $C_{24}Tet/C_{23}$ values could indicate a carbonate/evaporite source rock.

578 **Group 8**: BGR-6, -7, and -8 occur in the southwest TB in lagoonal facies. $\delta^{13}C$ isotopes
579 vary between -29 and -28 ‰. The oils were derived from algal-rich (high C_{27}/C_{29} sterane
580 ratios) clay/marl or evaporite, rather than carbonate, deposited in Ca2 lagoonal facies under
581 slightly reducing (HHI 0.13-0.14) and hypersaline depositional conditions (G/H 0.16 to 0.17).
582 C_{15} to C_{31} 2,3,6-aryl isoprenoids are present and isorenieratane – if at all – occurs only in
583 traces, which might be the result of relatively high thermal maturity (Table 2; Summons and
584 Powell, 1986). Elevated concentrations of C_{34} homohopanes over C_{33} and C_{35} homologues are
585 characteristic of the Group 8 oils.

586 **Group 9**: PL-4, -5, -12, -13 and 21 occur in NW Poland in lower slope/shallow-basin
587 facies. They are characterised by the lightest $\delta^{13}C$ isotopes (~-31 and -30 ‰). The source
588 rock for Group 9 received more clay/marl or evaporite than carbonate input, along with a
589 significant algal source (abundant C_{27} steranes) located in Ca2 lower slope/shallow-basin
590 facies deposited under reducing and hypersaline conditions. Chlorobactane, isorenieratane or
591 β-isorenieratane were not detected (Fig. 6). Elevated concentrations of C_{32} and C_{35}
592 homohopanes over lower and higher homologues are characteristic of this group. PL-4 and -5
593 oils, which are reservoired in Ca3 basin (dolo-mudstone and anhydrite) facies, have
594 biomarker characteristics similar to Ca2 oils in this group which suggests that Ca3 oils may
595 have been generated and migrated from Ca2 lower slope/shallow-basin facies.

596 **Group 10**: PL-10, -14, -17 occur in SW Poland in inner shoal/lagoonal facies. They are
597 similar to Group 1 but have less depleted $\delta^{13}C$ isotopes (-26.6 to -25.6 ‰). Group 10 is
598 characterised by an almost even percentage of $C_{33\text{-}35}$ homohopanes. The oils were derived
599 from microbial-rich source rocks deposited under anoxic/euxinic (HHI 0.16-0.18, BNH/H
600 0.02-0.05, isorenieratane 141-341 µg g^{-1} oil, chlorobactane 6-14 µg g^{-1} oil) conditions in Ca2
601 hypersaline lagoons.

602

603 **7. Conclusions**

604 As is the case for petroleum systems in general, Zechstein reservoirs are heterogeneous
605 and an in-depth understanding would be possible only after detailed examination of a much
606 larger dataset. Such attempts were beyond the scope of this paper and, furthermore, complete
607 datasets on the individual systems were not available. However, from the available dataset we
608 have integrated a suite of various biomarker parameters in order to interpret redox conditions

and OM source for Ca2 oils. Thirty-nine Zechstein Main Dolomite oils were analysed to investigate their origin in the eastern and south-central sector of the Southern Permian Basin of Europe. The investigated Ca2 oil samples reveal 10 groups based on their stable carbon isotopes, biomarker fingerprints and subtle biomarker differences. The oils show strong geochemical similarity within these particular groups and in some cases, sharp differences among them. The thermal maturity of the studied oils corresponds to the peak to late oil window, the latter being difficult to interpret with respect to source.

The biomarker correlations between the Ca2 oils revealed that the very high DBT/P and sterane ratios can be used for thermal maturity assessments for Zechstein Main Dolomite oils. With respect to source, these biomarker data indicate that the oils were derived from evaporite- and carbonate- rich source rocks (i.e., the Main Dolomite and overlying and underlying evaporites) deposited under marine conditions and characterized by a significant contribution of sapropelic (algal + microbial) OM and a subordinate clay(marl)-associated OM. Source rocks for Groups 6 and 7 oils could not be clearly determined due to their high thermal maturity and low abundance of source-specific biomarkers, although high C_{24}Tet/C_{23} values suggest a carbonate-evaporite depositional environment for their source rocks as well. Importantly, some characteristic biomarkers allowed more nuanced identification of source facies; for example, C_{40} aromatic carotenoids are particularly distinct among oils, and isorenieratene derivatives were used for oil groupings, for the first time to the best of our knowledge. Collectively, this allowed the identification of the 10 distinct groups, defined by depositional environment, geographical location in the SPB, OM source and thermal maturity.

Acknowledgements

We dedicate this paper to the memory of Dr Cezary Grelowski (†), an excellent petroleum geochemist. After finishing his studies he worked in the Piła Branch of the Polish Oil and Gas Company (PGNiG SA) for the rest of his life. Being fascinated with his work and new geochemical concepts, Cezary was a fantastic partner in the field and laboratory. Having a predisposition to scientific work he would approach difficult problems with unconventionally disputing the erudition and profound knowledge of the matter. Dr Cezary Grelowski was a cordial, obliging, friendly person, and remained an optimist, never despairing in his work on his passion – organic geochemistry! His credo was knowledge, hard work and helpfulness, till the end, and as such a person he will remain in our memory.

We also dedicate this paper to Dr Franz Kockel (†), for his outstanding and successful engagement for developing collaboration between geoscientists from the Central European Basin area. Understanding geology is only possible in a holistic way – a basic principle exemplified by Franz Kockel. It was his heartfelt wish to share his experience in regional geology with colleagues from neighbouring countries, especially from Central Europe.

Some crude oil samples (Poland) were kindly obtained from GeoMark Research (Houston). Shell Exploration and Production is thanked for partial financial support and ENGIE for permission to publish the results. The study of some Polish oils has also been financially supported by a statutory research project (no. 11.11.140.626) granted by the AGH University of Science and Technology, Kraków. We thank Jürgen Poggenburg for discussion, Monika Weiß, Adam Kowalski, James Williams and Alison Kuhl for help with instruments. We also wish to thank the Natural Environment Research Council (NERC), UK, for partial funding of the mass spectrometry facilities at Bristol (contract no. R8/H10/63). Finally, we acknowledge constructive and helpful comments of an associate editor Barry J. Katz, Benedikt Lerch, Joseph Curiale and two anonymous reviewers, which improved the quality of our manuscript. M.S. was supported by a Mobility Plus programme post-doctoral fellowship of the Ministry of Science and Higher Education of Poland and Shell Exploration and Production. R.D.P. acknowledges the Royal Society Wolfson Research Merit Award (UK).

References

Albrecht, H., 1932. Die Erdöllagerstätte Volkenroda. Zeitschrift der Deutschen Geologischen Gesellschaft 84, 361-363.

Andrusevich, V.E., Engel. M.H., Zumberge, J.E., Brothers, L.A., 1998. Secular episodic changes in stable carbon isotope composition of crude oils. Chemical Geology 152, 59-72.

Beach, F., Peakman, T.M., Abbott, G.D., Sleeman, R., Maxwell, J.R., 1989. Laboratory thermal alteration of triaromatic steroid hydrocarbons. Organic Geochemistry 14, 109-111.

Best, G., 1989. Die Grenze Zechstein/Buntsandstein in Nordwest-Deutschland nach Bohrlochmessungen. Zeitschrift der Deutschen Gesellschaft für Geowissenschaften 147, 455-464.

671 Blumenberg, M., Heunisch, C., Lückge, A., Scheeder, G., Wiese, F., 2016. Photic zone euxinia in the
672 central Rhaetian Sea prior the Triassic-Jurassic boundary. Palaeogeography, Palaeoclimatology,
673 Palaeoecology 461, 55-64.
674
675 Boon, J.J., Hine, S.H., Burlingame, A.L., Klok, J., Rijpstra, W.I.C., de Leeuw, J.W., Edmunds, K.E.,
676 Eglinton, G., 1983. Organic geochemical studies of Solar Lake laminated cyanobacterial mats. In:
677 Bjorøy, M., Albrecht, K., Cornford, K., de Groot, G., Eglinton, G., Galimov, E., Leythaeuser, D.,
678 Pelet, R., Rullkötter, J., Speers, G. (Eds.), Advances in Organic Geochemistry 1981. John Wiley &
679 Sons, New York, pp. 207–227.
680
681 Bousson, G., 1991. Relationship between different types of evaporitic deposits, and the occurrence of
682 organic-rich layers (potential source-rocks). Carbonate and Evaporites 6, 177-192.

683 Brosin, H. 2013. Die Erdölgewinnung in Thüringen - Von Anfang des 20. Jahrhunderts bis in die
684 1970er Jahre. Sonderheft der Beiträge zur Geologie von Thüringen, 154 pp.

685 Cao, C., Love, G.D., Hays, L.E., Wang, W., Shen, S., Summons, R.E., 2009. Biogeochemical
686 evidence for euxinic oceans and ecological disturbance presaging the end-Permian mass extinction
687 event. Earth and Planetary Science Letters 281, 188-201.

688 Chung, H.M., Rooney, M.A., Toon, M.B., Claypool, G.E., 1992. Carbon isotope composition of
689 marine crude oils. AAPG Bulletin 76, 1000-1007.

690 Clark, J.P., Philp, R.P., 1989. Geochemical characterization of evaporite and carbonate depositional
691 environments and correlation of associated crude oils in the Black Creek basin, Alberta. Bulletin of
692 Canadian Petroleum Geology 37, 401-416.

693 Connan, J., Cassou, A.M., 1980. Properties of gases and petroleum liquids derived from terrestrial
694 kerogen at various maturation levels. Geochimica et Cosmochimica Acta 44, 1-23.

695 Connan, J., Bouroullec, J., Dessort, D., Albrecht, P., 1986. The microbial input in carbonate-anhydrite
696 facies of a sabkha palaeoenvironment from Guatemala: a molecular approach. Organic Geochemistry
697 10, 29-50.

698 Connan, J., Dessort, D., 1987. Novel family of hexacyclic hopanoid alkanes (C_{32}-C_{35}) occurring in
699 sediments and oils from anoxic palaeoenvironments. Organic Geochemistry 11, 103-113.

700 Curiale, J.A., Cameron, D., Davis, D.V., 1985. Biological marker distribution and significance in oils
701 and rocks of the Monterey Formation, California. Geochimica et Cosmochimica Acta 49, 271-288.

Curiale, J.A., Odermatt, J.R., 1989. Short-term biomarker variability in the Monterey Formation, Santa Maria Basin. Organic Geochemistry 14, 1-13.

Curtis, J.B., Kotarba, M.J., Lewan, M.D., Więcław, D., 2004. Oil/source rock correlations in the Polish Flysch Carpathians and Mesozoic basement and organic facies of the Oligocene Menilite Shales: insights from hydrous pyrolysis experiments. Organic Geochemistry 35**,** 1573-1596.

Czechowski, F., Piela, J., 1997. Skład molekularny substancji organicznej zawartej w dolomicie głównym oraz skałach wylewnych z otworu Namyślin-1. Nafta-Gaz 53, 299-308.

Czechowski, F., Piela, J., Grelowski, C., Hojniak, M., Wojtkowiak, Z., Pikulski, L., 1998. Geochemiczne przesłanki ciągłości złoża gazu i ropy naftowej w rejonie Barnówko-Lubiszyn wynikające ze składu węglowodorów ciekłych w dolomicie głównym. Przegląd Geologiczny 46, 171-177.

da Cruz, F.G., de Vasconcellos, S.P., Angolini, C.F.F., Dellagnezze, B.M., Garcia, I.N.S., de Oliveira, V.M., dos Santos Neto, E.V., Marsaioli, A.J., 2011. Could petroleum biodegradation be a joint achievement of aerobic and anaerobic microrganisms in deep sea reservoirs? AMB Express 1, 47.

Defays, D., 1977. An efficient algorithm for a complete link method. The Computer Journal 20, 364-366.

Doornenbal, H., Stevenson, A., 2010. Petroleum geological atlas of the Southern Permian Basin area. EAGE Publication BV, 352 p.

Edgell, H.S., 1991. Proterozoic salt basins of the Persian Gulf area and their role in hydrocarbon generation. Precambrian Research 54, 1-14.

Farrimond, P., Bevan, J.C., Bishop, A.N., 1999. Tricyclic terpane maturity parameters: response to heating by an igneous intrusion. Organic Geochemistry 30, 1011-1019.

French, K.L., Rocher, D., Zumberge, J.E., Summons, R.E., 2015. Assessing the distribution of sedimentary C_{40} carotenoids through time. Geobiology 13, 139-151.

Frimmel, A., Oschmann, W., Schwark, L., 2004. Chemostratigraphy of the Posidonia Black Shale, SW Germany: I. Influence of sea-level variation on organic facies evolution. Chemical Geology 206, 199-230.

Fu, J., Sheng, G., Peng, P., Brassell, S.C., Eglinton, G., Jigang, J., 1986. Peculiarities of salt lake sediments as potential source rocks in China. Organic Geochemistry 10, 119–126.

731 Gąsiewicz, A., 2013. Climatic control on the Late Permian Main Dolomite (Ca2) deposition in
732 northern margin of the Southern Permian Basin and implications to its internal cyclicity. Geological
733 Society, London, Special Publications 376, 475-521.

734 Gerling, P., Piske, J., Rasch, H.-J., Wehner, H., 1996a. Paläogeograhie, Organofazies und Genese von
735 Kohlenwasserstoffen im Staβfurt-Karbonat Ostdeutschlands. 2. Genese von Erdölen und
736 Erdölbegleitgasen. Erdöl Erdgas Kohle 112, 152-156.

737 Gerling, P., Piske, J., Rasch, H.-J., Wehner, H., 1996b. Paläogeograhie, Organofazies und Genese von
738 Kohlenwasserstoffen im Staβfurt-Karbonat Ostdeutschlands. 1. Sedimentationsverlauf und
739 Muttergesteinsausbildung. Erdöl Erdgas Kohle 112, 13-18.

740 Grantham, P.J., 1986. The occurrence of unusual C_{27} and C_{29} sterane predominances in two types of
741 Oman crude oil. Organic Geochemistry 9, 1-10.

742 Grantham, P.J., Wakefield, L.L., 1988. Variations in the sterane carbon number distributions of
743 marine source rock derived crude oils through geological times. Organic Geochemistry 12, 61-77.

744 Grelowski, C., Czechowski, F., 2011. Diversity of source, biomarkers composition and maturity of
745 crude oils in Zechstein Main Dolomite deposits, NW Poland. 25th International Meeting on Organic
746 Geochemistry, 18-23 September, Interlaken, Switzerland. Book of abstracts, p. 242.

747 Grice, K., Schaeffer, P., Schwark, L., Maxwell, J.R., 1996. Molecular indicators of
748 palaeoenvironmental conditions in an immature Permian shale (Kupferschiefer, Lower Rhine Basin,
749 north-west Germany) from free and S-bound lipids. Organic Geochemistry 25, 131-147.

750 Grice, K., Schouten, S., Nissenbaum, A., Charrach, J., Sinninghe Damsté, J.S., 1998. Isotopically
751 heavy carbon in the C_{21} to C_{25} regular isoprenoids in halite-rich deposits from the Sdom Formation,
752 Dead Sea Basin, Israel. Organic Geochemistry 28, 349-359.
753 Hammes, U., Schulz, H.-M., Bechtel, A., 2014. Northern German unoonventional reservoirs in Upper
754 Permian (Ca2) microbial slope and basin dolomitized mudstones: assessment of oil to source-rock
755 correlations within a sequence stratigraphic framework. Search and Discovery Article #80238.

756 Hays, L.E., Grice, K., Foster, C.B., Summons, R.E., 2012. Biomarker and isotopic trends in a
757 Permian-Triassic sedimentary section at Kap Stosch, Greenland. Organic Geochemistry 43, 67-82.

758 Hiete, M., Berner, U., Heunisch, C., Röhling, H. 2005. A high resolution inorganic geochemical
759 profile across the Zechstein-Buntsandstein boundary in the North German Basin. Zeitschrift der
760 Deutschen Gesellschaft für Geowissenschaften 157, 77-106.

761 Hindenberg, K., 1999. Genese, Migration und Akkumulation von Erdöl in Mutter- und
762 Speichergesteinendes Staßfurt-Karbonat (Ca2) von Mecklenburg-Vorpommern und Südost-
763 Brandenburg. Bericht des FZ Jülich, No 3698, 184 pp.

764 Hofmann, P., Leythaeuser, D., 1995. Migration of hydrocarbons in carbonate source rocks of the
765 Staβfurt member (Ca2) of the Permian Zechstein, borehole Aue 1, Germany: the role of solution
766 seams. Organic Geochemistry 23, 597-606.

767 Hounslow, M.W., Balabanov, Y.P., *in press.* A geomagnetic polarity timescale for the Permian,
768 calibrated to stage boundaries. Geological Society, London, Special Publications 450,
769 https://doi.org/10.1144/SP450.8

770 Huang, W.-Y., Meinschein, W.G., 1979. Sterols as ecological indicators. Geochimica et
771 Cosmochimica Acta 43, 739-745.

772 Huang, D., Li, J., Zhang, D., 1990. Maturation sequence of continental crude oils in hydrocarbon
773 basins in China and its significance. Organic Geochemistry 16, 521-529.

774 Hughes, W.B., Holba, A.G., Dzou, L.I.P., 1995. The ratios of dibenzothiophene to phenanthrene and
775 pristane to phytane as indicators of depositional environment and lithology of petroleum source rocks.
776 Geochimica et Cosmochimica Acta 59, 3581-3598.

777 Jiamo, F., Guoying, S., Pingan, P., Brassell, S.C., Eglinton, G., Jigang, J., 1986. Peculiarities of salt
778 lake sediments as potential source rocks in China. Organic Geochemistry 10, 119-126.

779 Joachimski, M., Ostertag-Henning, C., Pancost, R.D., Strauss, H., Freeman, K.H., Littke, R.,
780 Sinninghe Damsté, J., Racki, G., 2001. Water column anoxia, enhanced productivity and concomitant
781 changes in $\delta^{13}C$ and $\delta^{34}S$ across the Frasnian-Famennian boundary (Kowala-Holy Cross
782 Mountains/Poland). Chemical Geology 175, 109-131.

783 Jurisch, A., Krooss, B.M., 2008. A pyrolytic study of the speciation and isotopic composition of
784 nitrogen in carboniferous shales of the North German Basin. Organic Geochemistry 39, 924-928.

785 Karnin, W.-D., Idiz, E., Merkel, D., Ruprecht, E., 1996. The Zechstein Stassfurt Carbonate
786 hydrocarbon system of the Thuringian Basin, Germany. Petroleum Geoscience 2, 53-58.

787 Katz, B.J., Elrod, L.W., 1983. Organic geochemistry of DSDP Site 467, offshore California, Middle
788 Miocene to Lower Pliocene strata. Geochimica et Cosmochimica Acta 47, 389-396.

789 Kenig, F., Hudson, J.D., Sinninghe Damsté, J.S., Popp, B.N., 2004. Intermittent euxinia:
790 reconciliation of a Jurassic black shale with its biofacies. Geology 32, 421-424.

791 Kirkland, D.W., Evans, R., 1981. Source-rock potential of evaporitic environment. AAPG Bulletin 65,
792 181-190.

793 Kodner, R.B., Pearson, A., Summons, R.E., Knoll, A.H., 2008. Sterols in red and green algae:
794 quantification, phylogeny, and relevance for the interpretation of geologic steranes. Geobiology 6,
795 411-420.

796 Koopmans, M.P., Köster, J., Van Kaam-Peters, H.M.E., Kenig, F., Schouten, S., Hartgers, W.A., de
797 Leeuw, J.W., Sinninghe Damsté, J.S., 1996. Diagenetic and catagenetic products of isorenieratene:
798 molecular indicators for photic zone anoxia. Geochimica et Cosmochimica Acta 60, 4467-4496.

799 Kosakowski, P., Krajewski, M., 2014. Hydrocarbon potential of the Zechstein Main Dolomite in the
800 western part of the Wielkopolska platform, SW Poland: New sedimentological and geochemical data.
801 Marine and Petroleum Geology 49, 99-120.

802 Kosakowski, P., Krajewski, M., 2015. Hydrocarbon potential of the Zechstein Main Dolomite (Upper
803 Permian) in western Poland: Relation to organic matter and facies characteristics. Marine and
804 Petroleum Geology 68, 675-694.

805 Kotarba, M.J., Koltun, Y.V., 2006. Origin and habitat of hydrocarbons of the Polish and Ukrainian
806 parts of the Carpathian Province. AAPG Memoir 84, 395-443.

807 Kotarba, M., Wagner, R., 2007. Generation potential of the Zechstein Main Dolomite (Ca2)
808 carbonates in the Gorzów Wielkopolski-Międzychód-Lubiatów area: geological and geochemical
809 approach to microbial-algal source rock. Przegląd Geologiczny 55, 1025-1036.

810 Kotarba, M., Więcław, D., Kowalski, A., 1998. Geneza gazu ziemnego i ropy naftowej z wybranych
811 obszarów basenu dewońskiego i cechsztyńskiego Niżu Polskiego w świetle badań geochemicznych.
812 Prace Państwowego Instytutu Geologicznego 165, 261-272.

813 Kotarba, M., Więcław, D., Kowalski, A., 2000. Skład, geneza i środowisko generowania ropy
814 naftowej w utworach dolomitu głównego zachodniej części obszaru przedsudeckiego. Przegląd
815 Geologiczny 48, 436-442.

816 Kotarba, M., Kosakowski, P., Więcław, D., Kowalski, A., 2003. Potencjał naftowy utworów dolomitu
817 głównego w strefie Kamienia Pomorskiego. Część 1 – Macierzystość. Przegląd Geologiczny 51, 587-
818 594.

819 Kotarba, M.J., Więcław, D., Koltun, Y.V., Marynowski, L., Kuśmierek, J., Dudok, I.V., 2007.
820 Organic geochemical study and genetic correlation of natural gas, oil and Menilite source rocks in the

area between San and Stryi rivers (Polish and Ukrainian Carpathians). Organic Geochemistry 38, 1431–1456.

Kotarba, M.J., Bilkiewicz, E., Hałas, S., 2017. Mechanisms of generation of hydrogen sulphide, carbon dioxide and hydrocarbon gases from selected petroleum fields of the Zechstein Main Dolomite carbonates of the western part of Polish Southern Permian Basin: Isotopic and geological approach. Journal of Petroleum Science and Engineering 157, 380-391.

Krooss, B.M., Littke, R., Müller, B., Frielingsdorf, J., Schwochau, K., Idiz, E.F., 1995. Generation of nitrogen and methane from sedimentary organic matter: Implications on the dynamics of natural gas accumulations. Chemical Geology 126, 291-318.

Krooss, B.M., Friberg, L., Gensterblum, Y., Hollenstein, J., Prinz, D., Littke, R., 2005. Investigation of the pyrolytic molecular nitrogen from Palaeozoic sedimentary rocks. International Journal of Earth Sciences 94, 1023-1038.

Krooss, B.M., Jurisch, A., Plessen, B., 2006. Investigation of the fate of nitrogen in Palaeozoic shales of the Central European Basin. Journal of Geochemical Exploration 89, 191-194.

Lott, G., Wong, T., Dusar, M., Andsbjerg, J., Mönning, E., Feldman-Olszewska, A., Verreussel, R., 2010. Jurassic. In: Doornenbal, J.C., Stevenson, A.G. (ed.), Petroleum geological atlas of the Southern Permian Basin area Eage Publications b.v. (Houten), p. 175-193.

Mello, M.R., Telnaes, N., Gaglianone, P.C., Chicarelli, M.I., Brassell, S.C., Maxwell, J.R., 1988a. Organic geochemical characterisation of depositional palaeoenvironments of source rocks and oils in Brazilian marginal basins. Organic Geochemistry 13, 31-45.

Mello, M.R., Gaglianone, P.C., Brassell, S.C., Maxwell, J.R., 1988b. Geochemical and biological marker assessment of depositional environments using Brazilian offshore oils. Marine and Petroleum Geology 5, 205–223.

Mello, M.R., Koutsoukos, E.A.M., Hart, M.B., Brassell, S.C., Maxwell, J.R., 1990. Late Cretaceous anoxic events in the Brazilian continental margin. Organic Geochemistry 14, 529–542.

Mikołajewski, Z., Czechowski, F., Grelowski, C., 2012. Charakterystyka geologiczno-litofacjalno-geochemiczna złóż ropy naftowej w utworach dolomitu głównego w rejonie platformy węglanowej Kamienia Pomorskiego. Prace Naukowe Instytutu Nafty i Gazu 182, 387–397.

Mingram, B., Hoth, P., Lüders, V., Harlov, D., 2005. The significance of fixed ammonium in Palaeozoic sediments for the generation of nitrogen-rich natural gases in the North German Basin. International Journal of Earth Sciences 94, 1010-1022.

852 Moldowan, J.M., Seifert, W.K., Gallegos, E.J., 1985. Relationship between petroleum composition
853 and depositional environment of petroleum source rocks. AAPG Bulletin 69, 1255-68.

854 Moldowan, J.M., Peters, K.E., Carlson, R.M.K., Schoell, M., Abu-Ali, M.A., 1994. Diverse
855 applications of petroleum biomarker maturity parameters. Arabian Journal for Science and
856 Engineering 19, 273-298.

857 Moldowan, J.M., Lee, C.Y., Watt, D.S., Jeganathan, A., Slougui, N.-E., Gallegos, E.J., 1991. Analysis
858 and occurrence of C_{26}-steranes in petroleum and source rocks. Geochimica et Cosmochimica Acta 55,
859 1065-1081.

860 Müller, E.P., 1984. Zur Genese von Erdölen in Karbonaten am Beispiel der Lagerstätten des Oberen
861 Perm des Territoriums der DDR. Zeitschrift für angewandte Geologie 30, 214-218.
862
863 Palacas, J.G., 1984. Carbonate rocks as sources of petroleum: geological and chemical characteristics
864 and oil-source correlations. Proceedings of the 11th World Petroleum Congress 1983, Vol. 2, John
865 Wiley & Sons, Chichester, UK, pp. 31–43.
866 Palacas, J.G., Anders, D.E., King, J.D., 1984. South Florida Basin – a prime example of carbonate
867 source rocks of petroleum. AAPG Studies in Geology 18, 71-96.
868 Paul, J., 2010. Zur Zyklizität und Dauer des Zechsteins. Zeitschrift der Deutschen Gesellschaft für
869 Geowissenschaften 161, 455-457.

870 Peryt, T.M., Geluk, M., Mathiesen, A., Paul, J., Smith, K., 2010. Zechstein. In: Doornenbal, J,.C.,
871 Stevenson, A.G. (eds), Petroleum Geological Atlas of the Southern Permian Basin Area. EAGE
872 Publications b.v. (Houten), p. 123-147.

873 Peters, K.E., Moldowan, J.M., 1991. Effects of source, thermal maturity, and biodegradation on the
874 distribution and isomerization of homohopanes in petroleum. Organic Geochemistry 17, 47-61.

875 Peters, K.E., Walters, C.C., Moldowan, J.M., 2005. The Biomarker Guide. Cambridge University
876 Press, Cambridge, 1155 pp.

877 Petersen, H.I., Hertle, M., Juhasz, A., Krabbe, H., 2016. Oil family typing, biodegradation and source
878 rock affinity of liquid petroleum in the Danish North Sea. Journal of Petroleum Geology 39, 247-268.

879 Pharaoh, T.C., Dusar, M., Geluk, M.C., Kockel, F., Krawczyk, C.M., Krzywiec, P., Schenk-
880 Wenderoth, M., Thybo, H., Vejbæk, van Wees, J.D., 2010. Tectonic evolution. In: Doornenbal, J.C.,
881 Stevenson, A.G. (eds), Petroleum Geological Atlas of the Southern Permian Basin Area. Eage
882 Publications b.v. (Houten), p. 25-57.

883 Philp, R.P., Chen, J.H., Fu, J.M., Sheng, G.Y., 1992. A geochemical investigation of crude oils and
884 source rocks from Biyang Basin, China. Organic Geochemistry 18, 933-945.

885 Pletsch, T., Appel, J., Botor, D., Clayton, C., Duin, E., Faber, E., Górecki, W., Kombrink, H.,
886 Kosakowski, P., Kuper, G., Kus, J., Lutz, R., Mathiesen, A., Ostertag-Henning, C., Papiernik, B., van
887 Bergen, F., 2010. Petroleum generation and migration. In: Doornenbal, J.C., Stevenson, A.G. (eds),
888 Petroleum Geological Atlas of the Southern Permian Basin Area. Eage Publications b.v. (Houten), p.
889 225-253.

890 Radke, M., 1988. Application of aromatic compounds as maturity indicators in source rocks and crude
891 oils. Marine and Petroleum Geology 5, 224-236.

892 Requejo, A.G., 1994. Maturation of petroleum source rocks—II. Quantitative changes in extractable
893 hydrocarbon content and composition associated with hydrocarbon generation. Organic Geochemistry
894 21: 91-105.

895 Richter-Bernburg, G., 1953. Stratigraphische Gliederung des deutschen Zechsteins. Zeitschrift der
896 Deutschen Geologischen Gesellschaft 105, 843-854.

897 Schoell, M., 1984. Wasserstoff- und Kohlenstoffisotope in organischen Substanzen, Erdölen und
898 Erdgassen. Geologische Jahrbuch D67, 167pp.

899 Schwark, L., Vliex, M., Karnin, W.-D., Waldmann, R., 1998. Geochemische Untersuchungen an
900 ausgewählten Mutter- und Speichergesteinen des Zechsteins am Beispiel der Bohrung Sprötau Z1
901 (Thüringen Becken). Geologische Jahrbuch A149, 185-211.

902 Seifert, W.K., Moldowan, J.M., 1978. Applications of steranes, terpanes and monoaromatics to the
903 maturation, migration and source of crude oils. Geochimica et Cosmochimica Acta 42, 77-95.

904 Seifert, W.K., Moldowan, J.M., 1979. The effect of biodegradation on steranes and terpanes in crude
905 oils. Geochimica et Cosmochimica Acta 43, 111-126.

906 Seifert, W.K., Moldowan, J.M., 1986. Use of biological markers in petroleum exploration. Methods in
907 Geochemistry and Geophysics 24, 261-290.

908 Shanmugam, G., 1985. Significance of coniferous rain forest and related organic matter in generating
909 commercial quantities of oils, Gippsland Basin, Australia. AAPG Bulletin 69, 1241-1254.

910 Simoneit, B.R., Schoell, M., Dias, R.F., de Aquino Neto, F.R., 1993. Unusual carbon isotope
911 compositions of biomarker hydrocarbons in a Permian tasmanite. Geochimica et Cosmochimica Acta
912 57, 4205-4211.

913 Sinninghe Damsté, J.S., Wakeham, S.G., Kohnen, M.E.L., Hayes, J.M., de Leeuw, J.W., 1993. A
914 6,000-year sedimentary molecular record of chemocline excursions in the Black Sea. Nature 362,
915 827-829.

916 Sinninghe Damsté, J.S., Van Duin, A.C.T., Hollander, D., Kohnen, M.E.L., de Leeuw, J.W., 1995a.
917 Early diagenesis of bacteriohopanepolyol derivatives: formation of fossil homohopanoids.
918 Geochimica et Cosmochimica Acta 59, 5141-5155.

919 Sinninghe Damsté, J.S., Kenig, F., Koopmans, M.P., Köster, J., Schouten, S., Hayes, J.M, de Leeuw,
920 J.W., 1995b. Evidence for gammacerane as an indicator of water column stratification. Geochimica et
921 Cosmochimica Acta 59, 1895-1900.

922 Słowakiewicz, M., Mikołajewski, Z., 2009. Sequence stratigraphy of the Upper Permian Zechstein
923 Main Dolomite carbonates in western Poland: a new approach. Journal of Petroleum Geology 32,
924 215-234.

925 Słowakiewicz, M., Mikołajewski, Z., Sikorska, M., Poprawa, P., 2010. Origin of diagenetic fluids in
926 the Zechstein Main Dolomite reservoir rocks, West Pomerania, Poland. Zeitschrift der Deutschen
927 Gesellschaft für Geowissenschaften 161, 25-38.

928 Słowakiewicz, M., Mikołajewski, Z., 2011. Upper Permian Main Dolomite microbial carbonates as
929 potential source rocks for hydrocarbons (W Poland). Marine and Petroleum Geology 28, 1572-1591.

930 Słowakiewicz, M., Gąsiewicz, A., 2013. Palaeoclimatic imprint, distribution and genesis of Zechstein
931 Main Dolomite (Upper Permian) petroleum source rocks in Poland: Sedimentological and
932 geochemical rationales. Geological Society, London, Special Publications 376, 523-538.

933 Słowakiewicz, M., Tucker, M.E., Pancost, R.D., Perri, E., Mawson, M., 2013. Upper Permian
934 (Zechstein) microbialites: Supratidal through deep subtidal deposition, source rock, and reservoir
935 potential. AAPG Bulletin 97, 1921-1936.

936 Słowakiewicz, M., Tucker, M.E., Perri, E., Pancost, R.D., 2015. Nearshore euxinia in the photic zone
937 of an ancient sea. Palaeogeography, Palaeoclimatology, Palaeoecology 426, 242-259.

938 Słowakiewicz, M., 2016. Characteristic biomarkers in organic matter from three Zechstein (Late
939 Permian) carbonate units. Zeitschrift der Deutschen Gesellschaft für Geowissenschaften 167, 269-279.

940 Słowakiewicz, M., Tucker, M.E., Hindenberg, K., Mawson, M., Idiz, E.F., Pancost, R.D., 2016a.
941 Nearshore euxinia in the photic zone of an ancient sea: Part II – The bigger picture and implications
942 for understanding ocean anoxia. Palaeogeography, Palaeoclimatology, Palaeoecology 461, 432-448.

943 Słowakiewicz, M., Perri, E., Tucker, M.E., 2016b. Micro- and nanopores in tight Zechstein 2
944 Carbonate facies from the Southern Permian Basin, NW Europe. Journal of Petroleum Geology 39,
945 149-168.

946 Sofer, Z., 1984. Stable carbon isotope compositions of crude oils: application to source depositional
947 environments and petroleum alteration. AAPG Bulletin 68, 31-49.

948 Sonnenfeld, P., 1985. Evaporites as oil and gas source rocks. Journal of Petroleum Geology 8, 253-
949 271.

950 Summons, R.E., Powell, T., 1986. Chlorobiaceae in Palaeozoic seas revealed by biological markers,
951 isotopes and geology. Nature 319, 763-765.

952 Szurlies, M., 2013. Late Permian (Zechstein) magnetostratigraphy in Western and Central Europe.
953 Geological Society, London, Special Publications 376, 73-85.

954 Taylor, J.C.M., 1998. Upper Permian – Zechstein. In: Glennie, K.W. (ed.), Petroleum geology of the
955 North Sea. Blackwell Science, 4th edition, 174-212.

956 Ten Haven, H.L., de Leeuw, J.W., Sinninghe Damsté, J.S., Schenck, P.A., Palmer, S.E., Zumberge,
957 J.E., 1988. Application of biological markers in the recognition of palaeohypersaline environments.
958 In: Fleet, A.J., Kelts, K., and Talbot, M.R. (ed.), Lacustrine petroleum source rocks. Geological
959 Society London, Special Publications 40, 123-130.

960 van Kaam-Peters, H.M.E., Rijpstra, W.I.C., de Leeuw, J.W., Sinninghe Damsté, J.S., 1998. A high
961 resolution biomarkers study of different lithofacies or organic sulfur-rich carbonate rocks of a
962 Kimmeridgian lagoon (French southern Jura). Organic Geochemistry 28, 151-177.

963 Volkman, J., 1986. A review of sterol markers for marine and terrigenous organic matter. Organic
964 Geochemistry 9, 83-99.

965 Volkman, J., Barrett, S., Blackburn, S., Mansour, M., Sikes, E., Gelin, F., 1998. Microalgal
966 biomarkers: a review of recent research development. Organic Geochemistry 29, 1163-1180.

967 Van Graas, G.W., 1990. Biomarker maturity parameters for high maturities: Calibration of the
968 working range up to the oil/condensate threshold. Organic Geochemistry 16, 1025-1032.

969 Van Wees, J.-D., Stevenson, R.A., Ziegler, P.A., McCann, T., Dadlez, R., Gaupp, R., Narkiewicz, M.,
970 Bitzer, F., Scheck, M., 2000. On the origin of the Southern Permian Basin, Central Europe. Marine
971 and Petroleum Geology 17, 43-49.

Wagner, R., 2012. Mapa paleogeograficzna dolomitu głównego (Ca2) w Polsce. Państwowy Instytut Geologiczny, unpublished.

Walters, C.C., Cassa, M.R., 1985. Regional organic geochemistry of offshore Louisiana. Gulf Coast Association of Geological Societies Transactions 35, 277-286.

Waples, D.W., Machihara, R., 1991. Biomarkers for geologists: a practical guide to the application of steranes and triterpanes in petroleum geology. AAPG Methods in Exploration Series 9, 91 pp.

Warren, J.K., 1986. Shallow water evaporitic environments and their source rock potential. Journal of Sedimentary Petrology 56, 442-454.

Warren, J.K., 2011. Evaporitic source rocks: mesohaline responses to cycles of 'famine or feast' in layered brines. IAS Special Publications 43, 315-392.

Wehner, H., 1997. Source and maturation of crude oils in northern and eastern Germany – an organic geochemical approach. Geologisches Jahrbuch D103, 85-102.

Zdanowski, P., Wozniak, K., 2010. Nitrogen source for the Main Dolomite natural gas in the Sulecin isolated platform area – verification of existing theory. 72nd EAGE Conference and Exhibition incorporating SPE EUROPEC 2010, J037.

Zhusheng, J., Philp, R.P., Lewis, C.A., 1988. Fractionation of biological markers in crude oils during migration and the effects on correlation and maturation parameters. Organic Geochemistry 13, 561-571.

Zumberge, J.E., Russell, J.A., Reid, S.A., 2005. Charging of Elk Hills reservoirs as determined by oil geochemistry. AAPG Bulletin 89, 1347-1371.

Captions to figures:

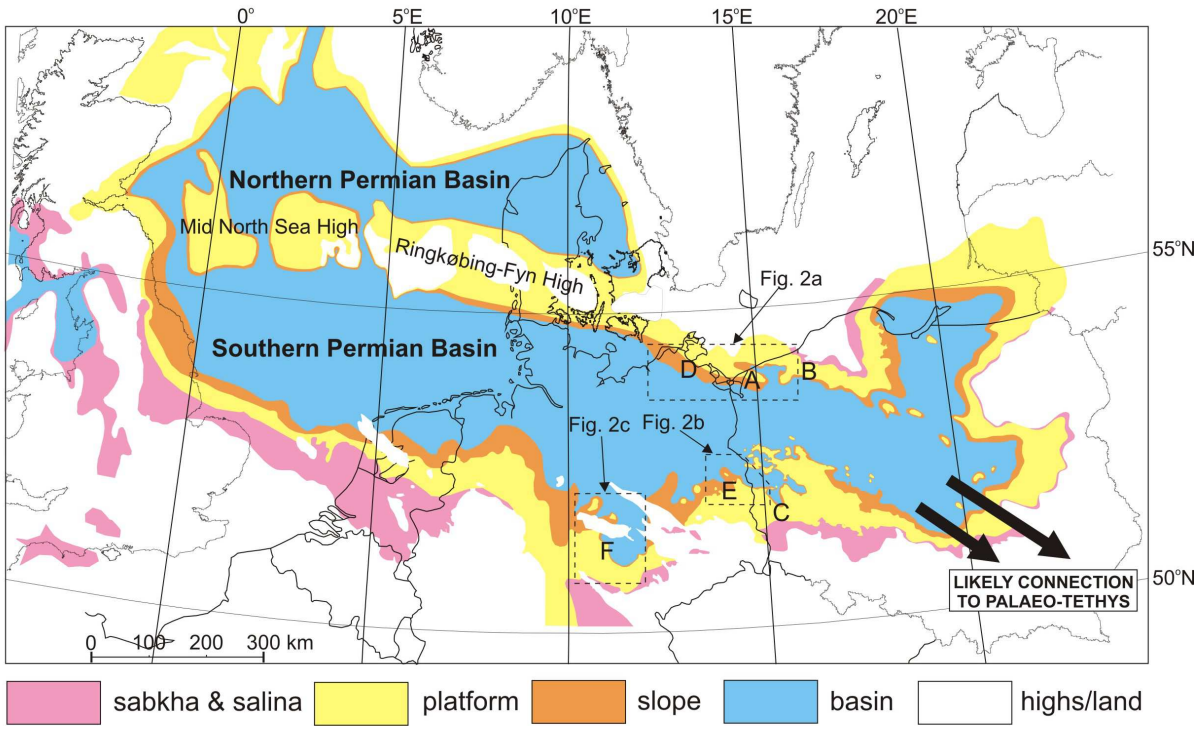

994

995 Fig. 1. Palaeoenvironmental map of the Ca2 in the Late Permian in Europe (updated after Słowakiewicz et al.,
996 2015). Longitude and latitude are present day values. A – Kamień Pomorski carbonate platform; B – Pomerania
997 carbonate platform; C – Fore-Sudetic Monocline; D – NE North German (sub)-Basin (Mecklenburg-
998 Vorpommern); E – SE North German (sub)-Basin (Brandenburg); F – Thuringian (sub)-Basin.

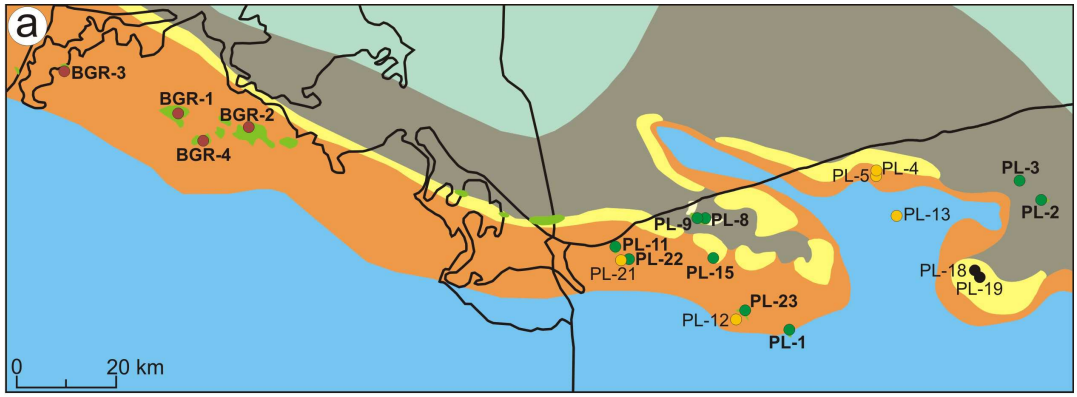

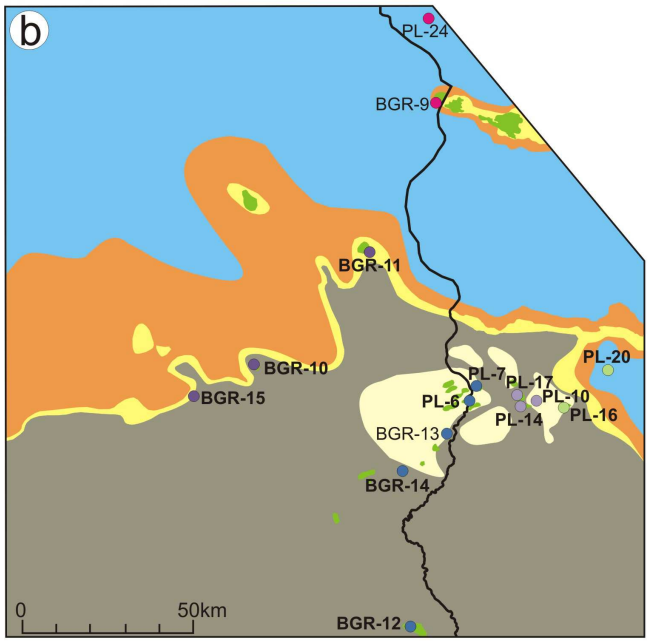

SYSTEM	LITHOSTRATIGRAPHY		
LATE PERMIAN	ZECHSTEIN	Z3	Y. Halite + Y. Potash
			Main Anhydrite (A3)
			Platy Dolomite (Ca3)
			Grey Pelite (T3)
		Z2	Screening Anhydrite (A2r)
			Screening Older Halite (Na2r)
			Older Potash (K2)
			Older Halite (Na2)
			Basal Anhydrite (A2)
			Main Dolomite (Ca2)
		Z1	Upper Anhydrite (A1b)
			Oldest Halite (Na1)
			Lower Anhydrite (A1a)
			Zechstein Limestone (Ca1)
			Kupferschiefer (T1)
	UPPER ROTLIEGEND		

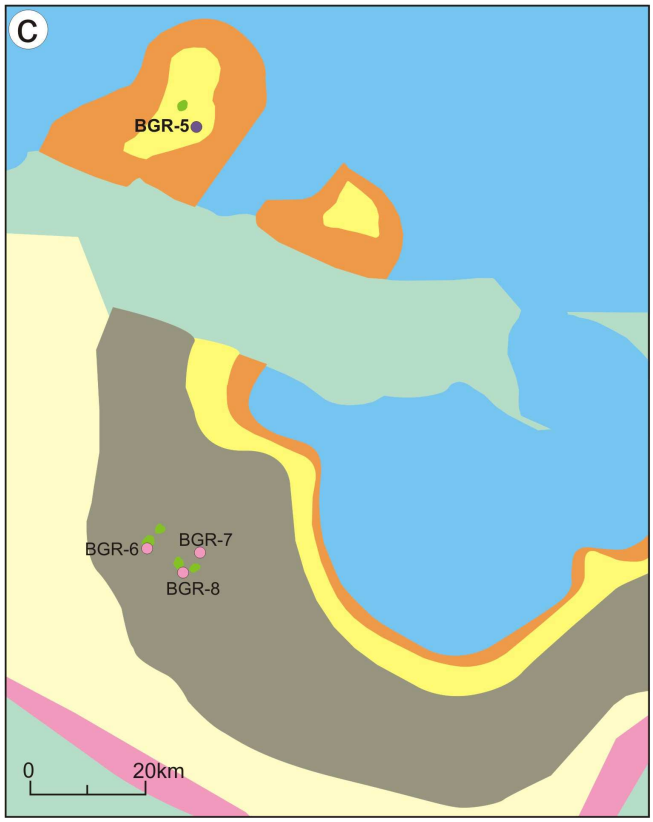

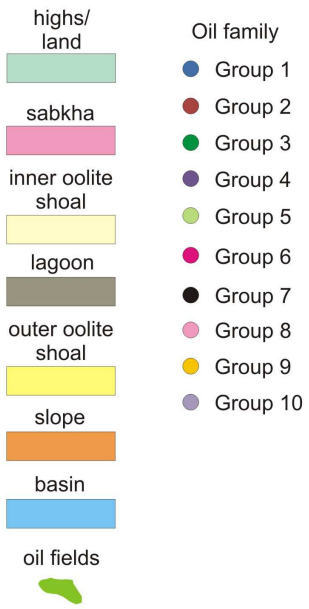

Fig. 2. Palaeoenvironmental maps, lithostratigraphy, and location of Ca2 oils in a) NW Poland and NE Germany; b) SW Poland and SE Germany; and c) Thuringian sub-basin, central-south Germany (modified after Hindenberg, 1999; Słowakiewicz et al., 2010; Brosin, 2013; Wagner, 2012; Gąsiewicz, 2013). Y. Halite + Y. Potash – Younger Halite (Na3) + Younger Potash (K3); Z1, Z2, Z3 – Zechstein cycles 1, 2, 3. Well names in bold font indicate crude oils containing isorenieratane.

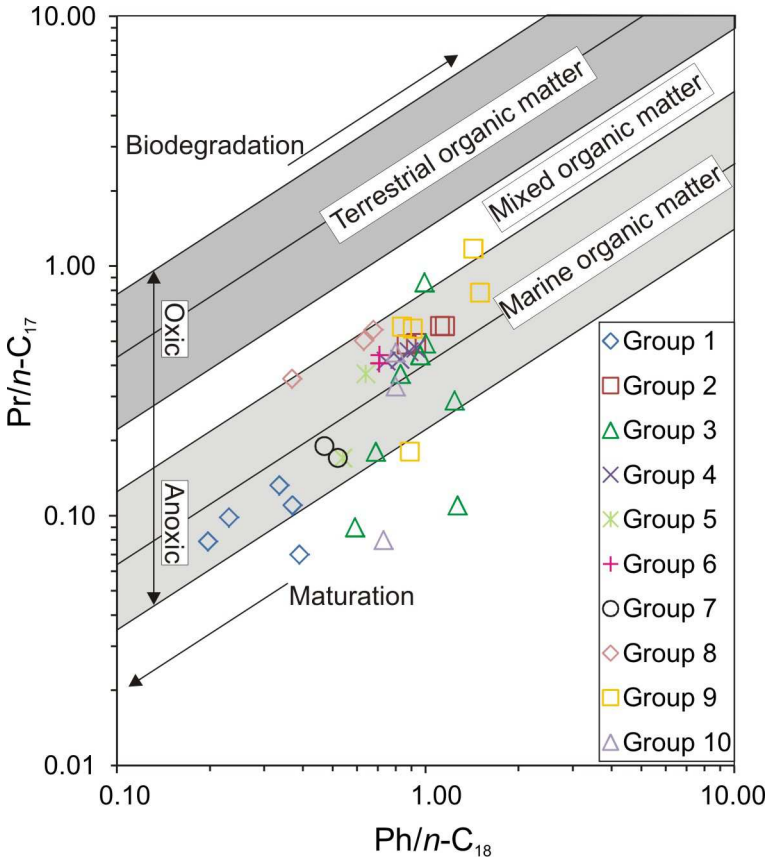

Fig. 3. Phytane to *n*-C_{18} alkane (Ph/*n*-C_{18}) versus pristane to *n*-C_{17} alkane (Pr/*n*-C_{17}) for Ca2 oil samples (graphical fields are according to Shanmugam, 1985).

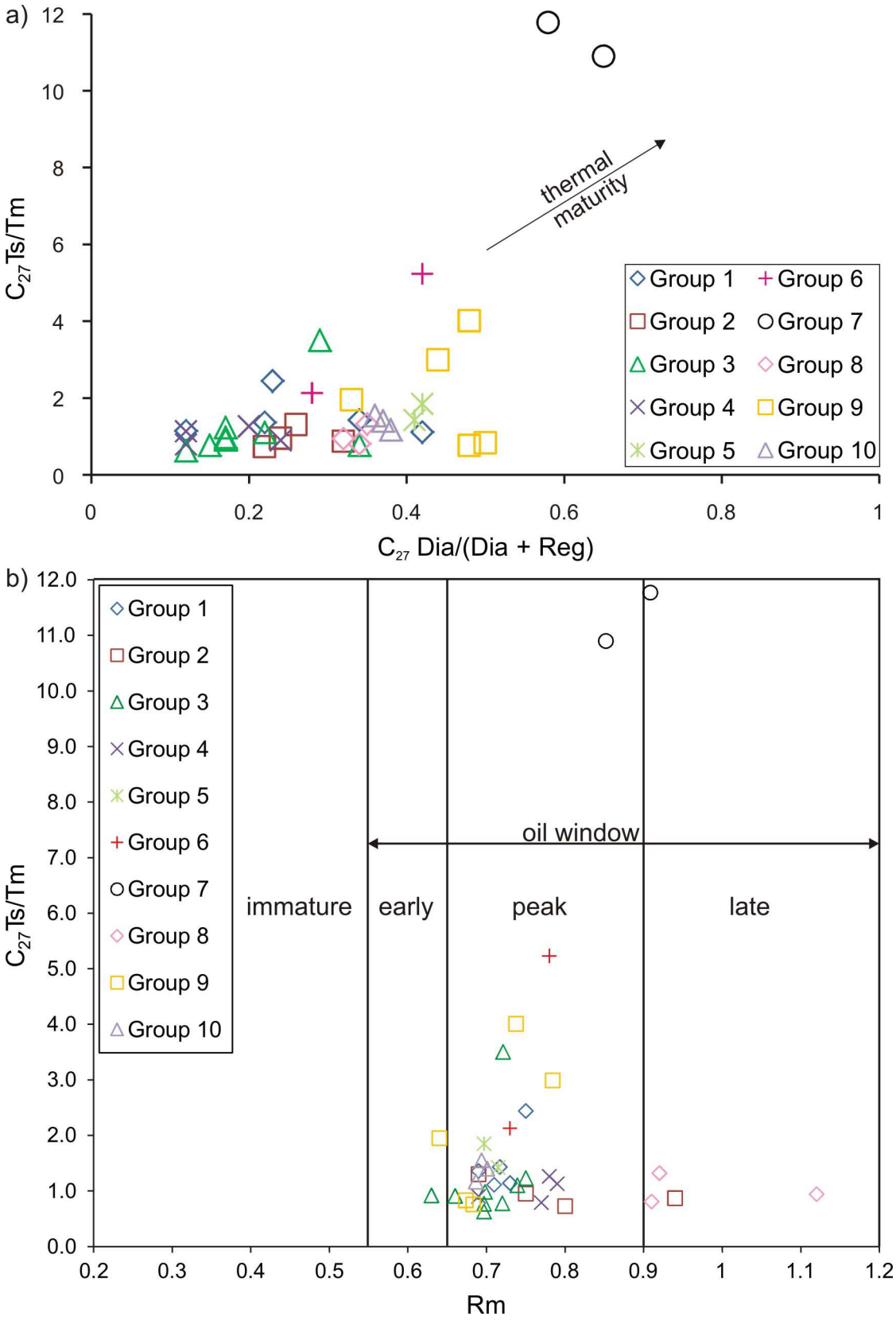

Fig. 4. C_{27} 18α-trisnorneohopane/17α-trisnorhopane (Ts/Tm) versus other geochemical ratios indicating thermal maturity of Ca2 oils. a) Ts/Tm versus C_{27} diasteranes/(diasteranes + regular steranes) [C_{27} Dia/(Dia + Reg)] shows thermal maturity control of Ca2 oil samples; b) Ts/Tm versus calculated vitrinite reflectance (Rm; Radke, 1988) grouping the majority of Ca2 oil samples within the peak oil window.

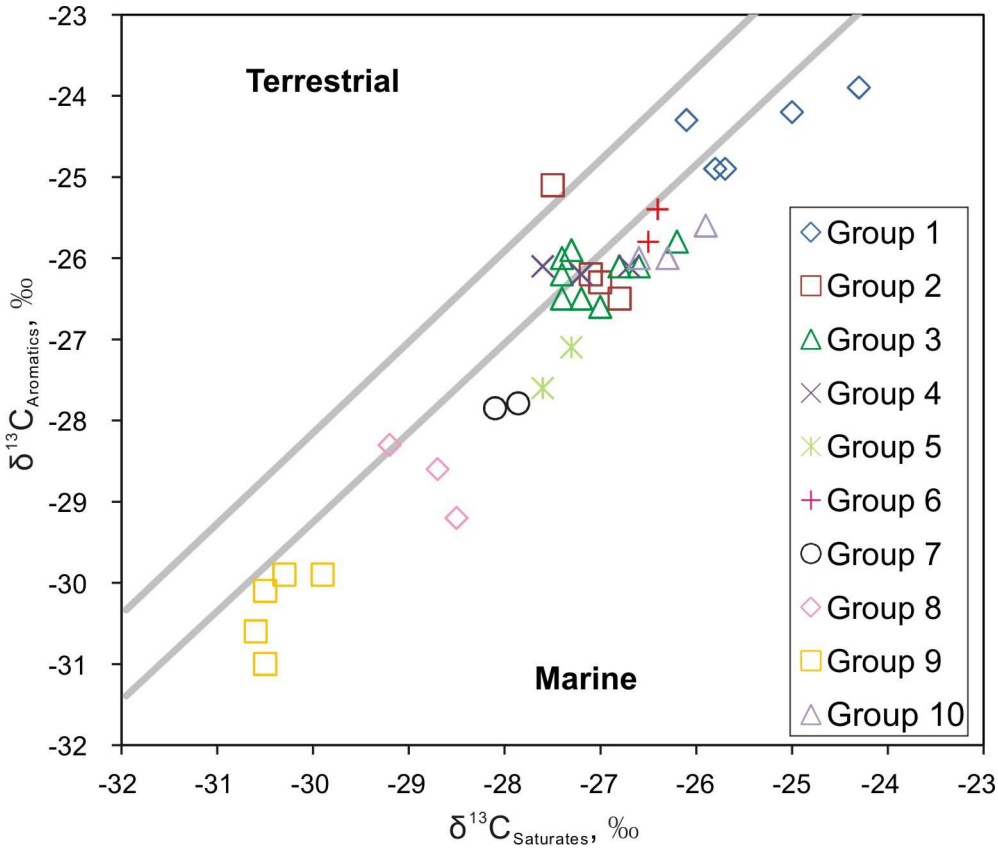

1013

1014 Fig. 5. Sofer's (1984) plot of $\delta^{13}C$ values for the saturated and aromatic fractions for Ca2 oils located in
1015 Germany and Poland.

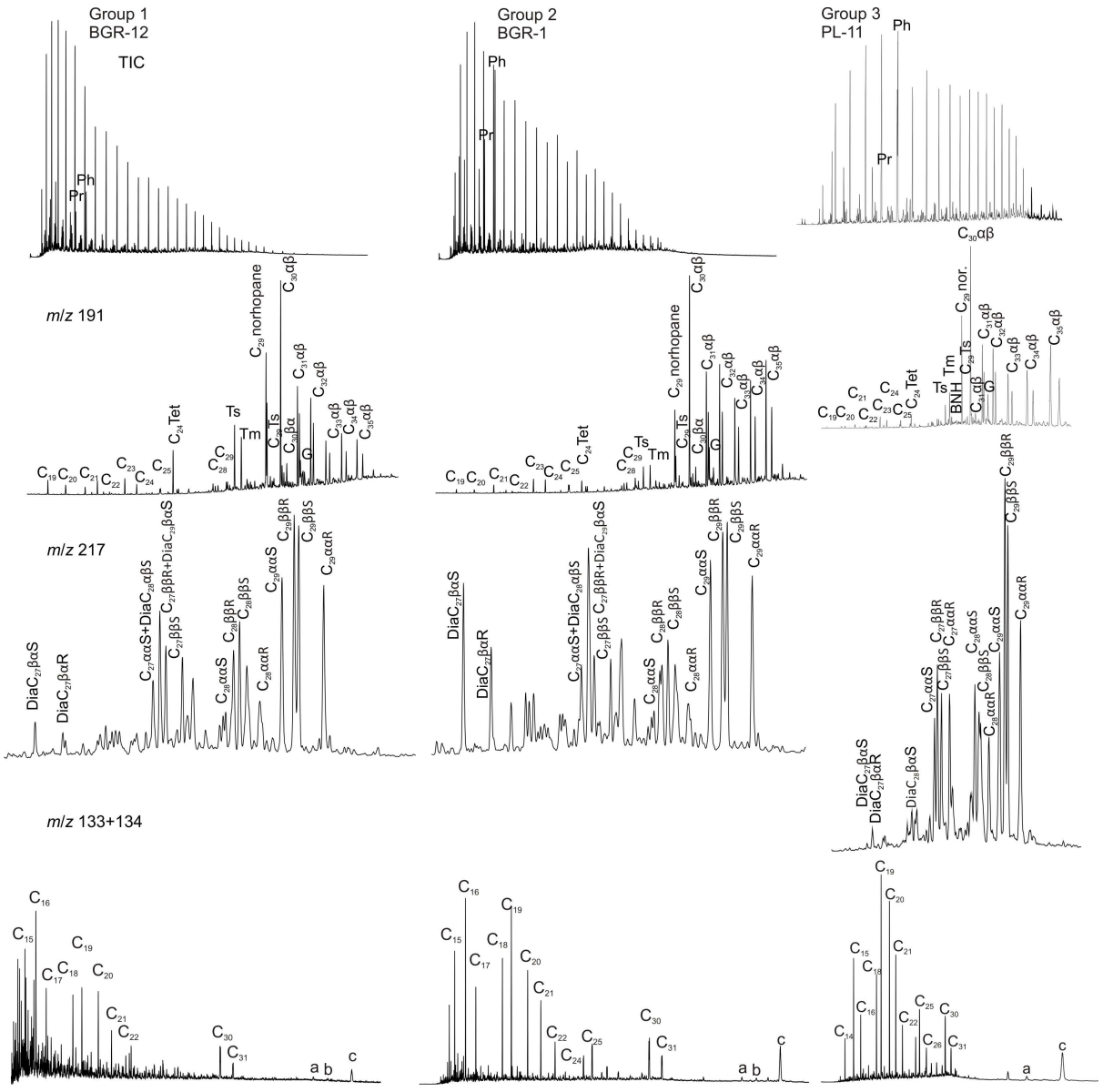
Group 1
BGR-12
TIC
Ph
Pr
Group 2
BGR-1
Ph
Pr
Group 3
PL-11
Ph
Pr
C30αβ
m/z 191
C29 norhopane
C30αβ
C24 Tet
Ts
Tm
C29
C28
C29 Ts
C30βα
G
C31αβ
C32αβ
C33αβ
C34αβ
C35αβ
C29 nor.
BNH
C19 C20 C21 C22 C23 C24 C25
m/z 217
DiaC27βαS
DiaC27βαR
C27ααS+DiaC28αβS
C27ββS
C27ββR+DiaC29βαS
C28ββR
C28ββS
C28ααS
C29ααR
C29ααS
C29ββR
C29ββS
C29ααR
C28ααR
C28ββR
C28ββS
C26ααR
C26ααS
C27ββS
C27ααR
C28βββS
C28βββR
C29βββS
C29βββR
m/z 133+134
C15
C16
C17
C18
C19
C20
C21
C22
C24
C25
C26
C30
C31
a
b
c

1016

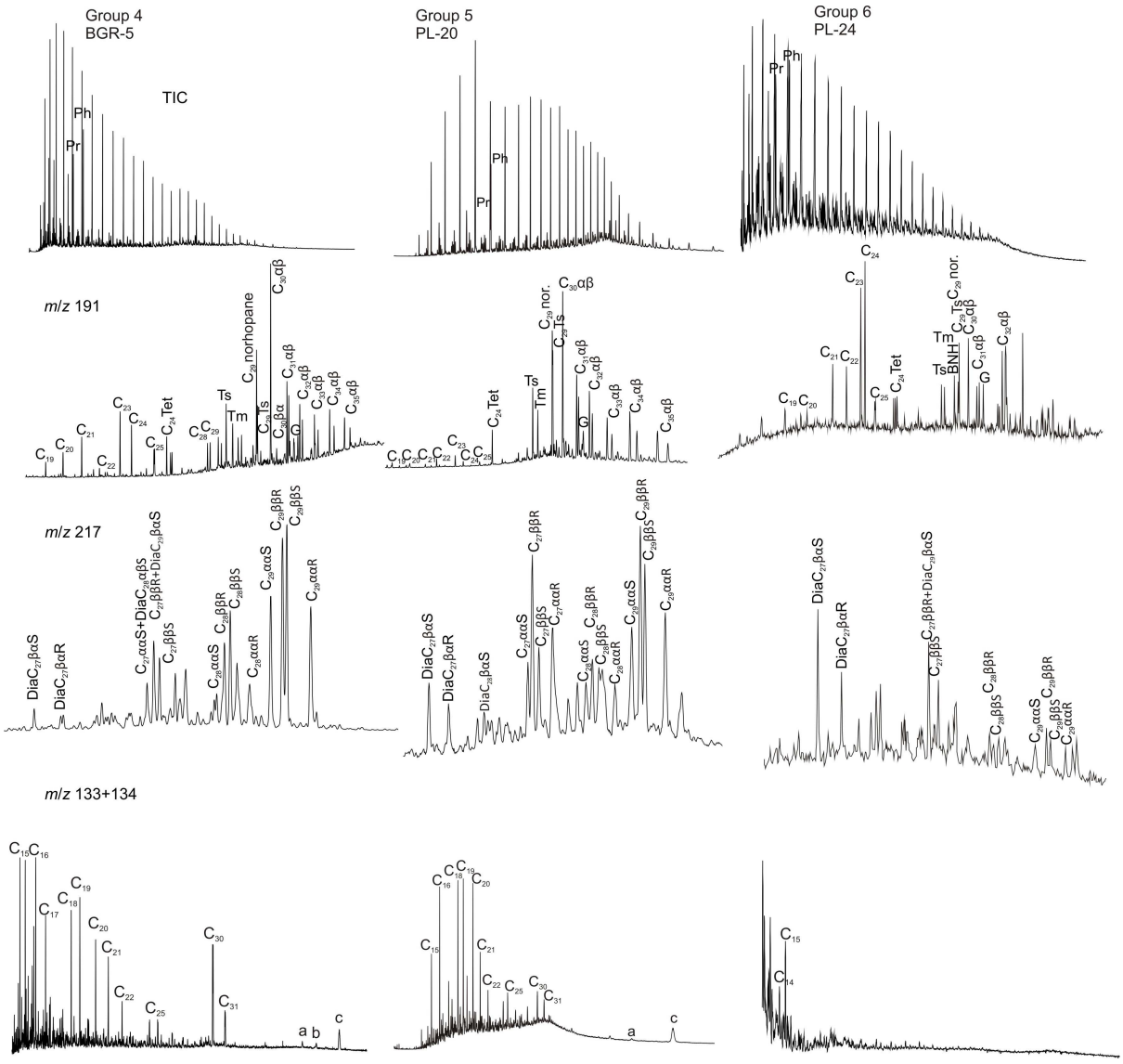
Group 4
BGR-5
TIC
Ph
Pr
Group 5
PL-20
Ph
Pr
Group 6
PL-24
Ph
Pr
m/z 191
C19
C20
C21
C22
C23
C24
C24 Tet
C25
C28
C29
Ts
Tm
C29 norhopane
C30αβ
C31αβ
C32αβ
C33αβ
C34αβ
C35αβ
G
C29 nor.
C29 Ts
C26αβ
BNH
m/z 217
DiaC27βαS
DiaC27βαR
C27αααS+DiaC28αβS
C27ββR+DiaC28βαS
C27ββS
C28ββR
C28ββS
C28αααS
C28αααR
C29ββR
C29ββS
C29αααR
C27αααS
C27ββR
C27ββS
C27αααR
C28αααS
C28ββS
C28αααR
C29αααS
C29ββR
C29ββS
C29αααR
DiaC27βαS
DiaC27βαR
C27ββS+DiaC29βαS
C28ββR
C29αααS
C29ββR
C29ββS
C29αααR
m/z 133+134
C15
C16
C17
C18
C19
C20
C21
C22
C25
C30
C31
a
b
c
C15
C16
C18
C19
C20
C21
C22
C25
C30
C31
a
c
C15
C14

1017

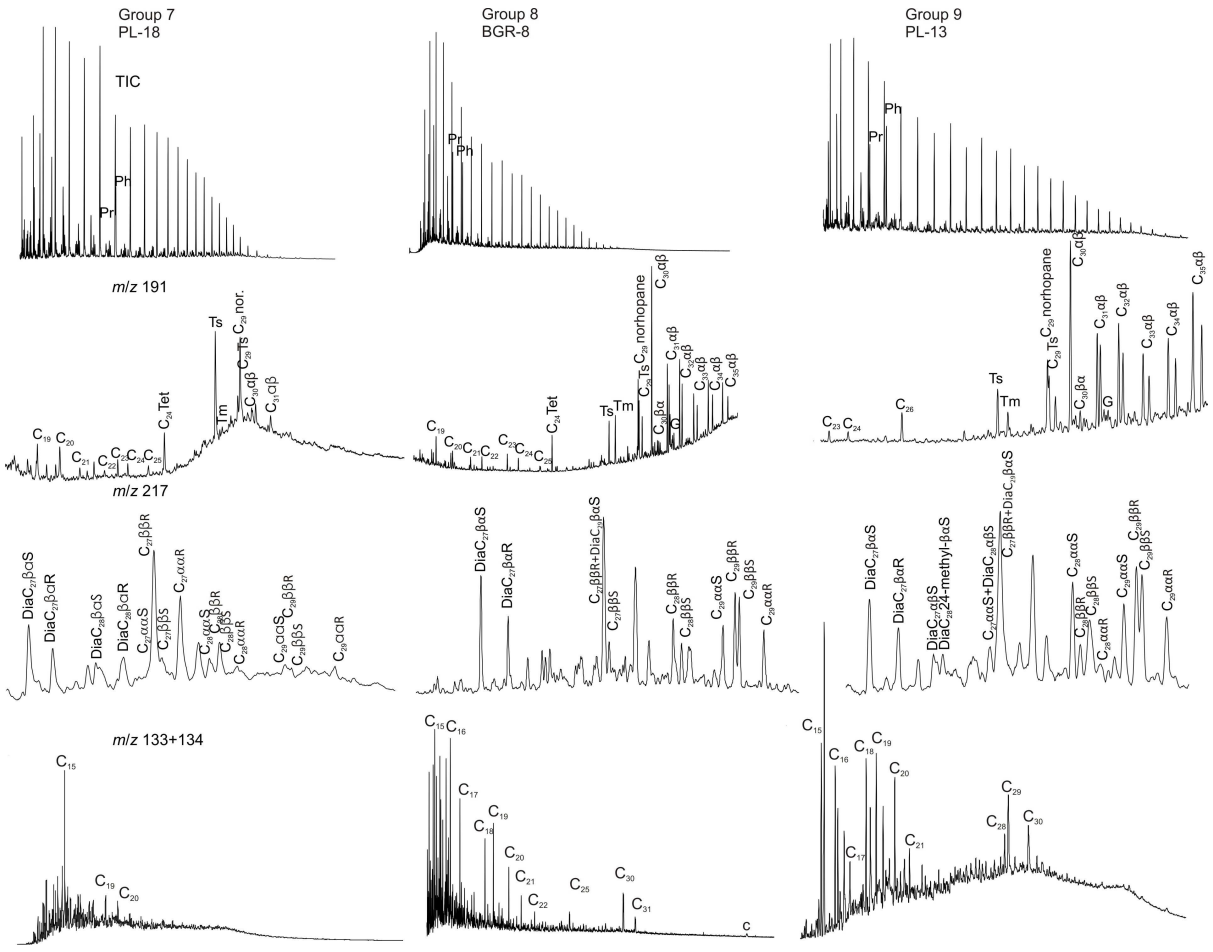
Group 7
PL-18
TIC
Ph
Pr
m/z 191
Ts
Tm
C29 nor.
C24 Tet
C19 C20 C21 C22 C23 C24 C25
C30αβ
C31αβ
m/z 217
DiaC27βαS
DiaC27βαR
DiaC28βαS
DiaC28βαR
C27ββR
C27ββS
C27ααR
C27αααS
C28ββR
C28ββS
C28ααR
C29ααS
C29ββR
C29ββS
C29ααR
m/z 133+134
C15
C19 C20
Group 8
BGR-8
Pr
Ph
C29 norhopane
C30αβ
C31αβ
C32αβ
C33αβ
C34αβ
C35αβ
Ts
Tm
C29βα
G
C24 Tet
C19 C20 C21 C22 C23 C24 C25
DiaC27βαS
DiaC27βαR
C27ββR+DiaC28ββR
C27ββS
C28ββR
C28ββS
C29ααS
C29ββR
C29ββS
C29ααR
C15 C16
C17
C18
C19
C20
C21
C22
C25
C30
C31
Group 9
PL-13
Ph
Pr
C29 norhopane
C30αβ
C31αβ
C32αβ
C33αβ
C34αβ
C35αβ
Ts
Tm
C29βα
G
C23 C24
C26
DiaC27βαS
DiaC27βαR
DiaC28-24-methyl-βαS
DiaC28αααS+DiaC28αββS
C27ββR+DiaC28βαS
C28ααS
C28ββR
C28ββS
C28ααR
C29ααS
C29ββR
C29ββS
C29ααR
C15
C16
C17
C18
C19
C20
C21
C26
C28
C29
C30

1018

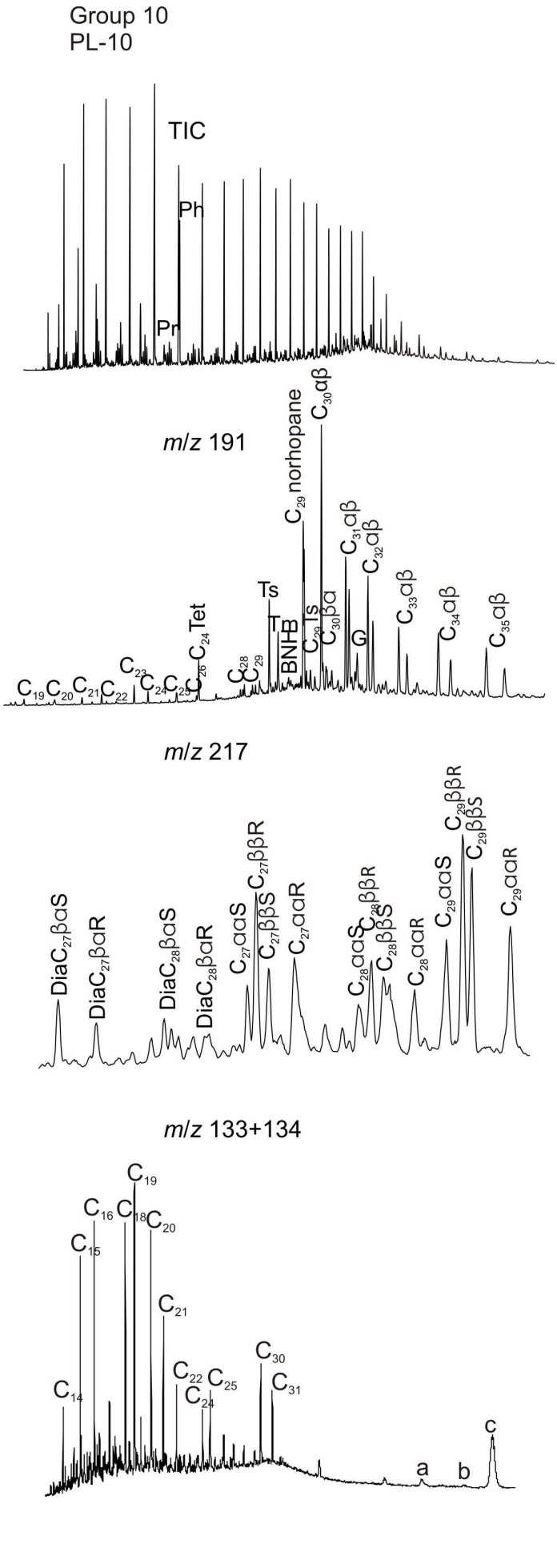
Group 10
PL-10
TIC
Ph
Pr
m/z 191
C29 norhopane
C30αβ
C31αβ
C32αβ
C33αβ
C34αβ
C35αβ
Ts
Tm
BNH
C29Ts
C30βα
G
C19 C20 C21 C22 C23 C24 C25 C26 Tet C24 C28 C29
m/z 217
DiaC27βαS
DiaC27βαR
DiaC28βαS
DiaC28βαR
C27ααS
C27βββR
C27βββS
C27ααR
C28ααS
C28βββR
C28βββS
C28ααR
C29ααS
C29βββR
C29βββS
C29ααR
m/z 133+134
C14
C15
C16
C18
C19
C20
C21
C22
C24
C25
C30
C31
a
b
c

Fig. 6. Representative total ion current chromatograms of whole oils (TIC) and mass chromatograms (*m/z* 191, *m/z* 217, *m/z* 133+134) of the saturated and aromatic fractions of Ca2 oils showing the correlation of ten oil groups. Ts – C_{27} 18α-trisnorneohopane; Tm - 17α-trisnorhopane; a – chlorobactane; b – *β*-isorenieratane; c – isorenieratane. Other symbols as in Table 1. Note that tricyclic terpanes in groups 6 and 7 have quite low abundance with respect to the overall high thermal maturity of the oil samples, which could result from the lithological type of the source rocks or alteration effects.

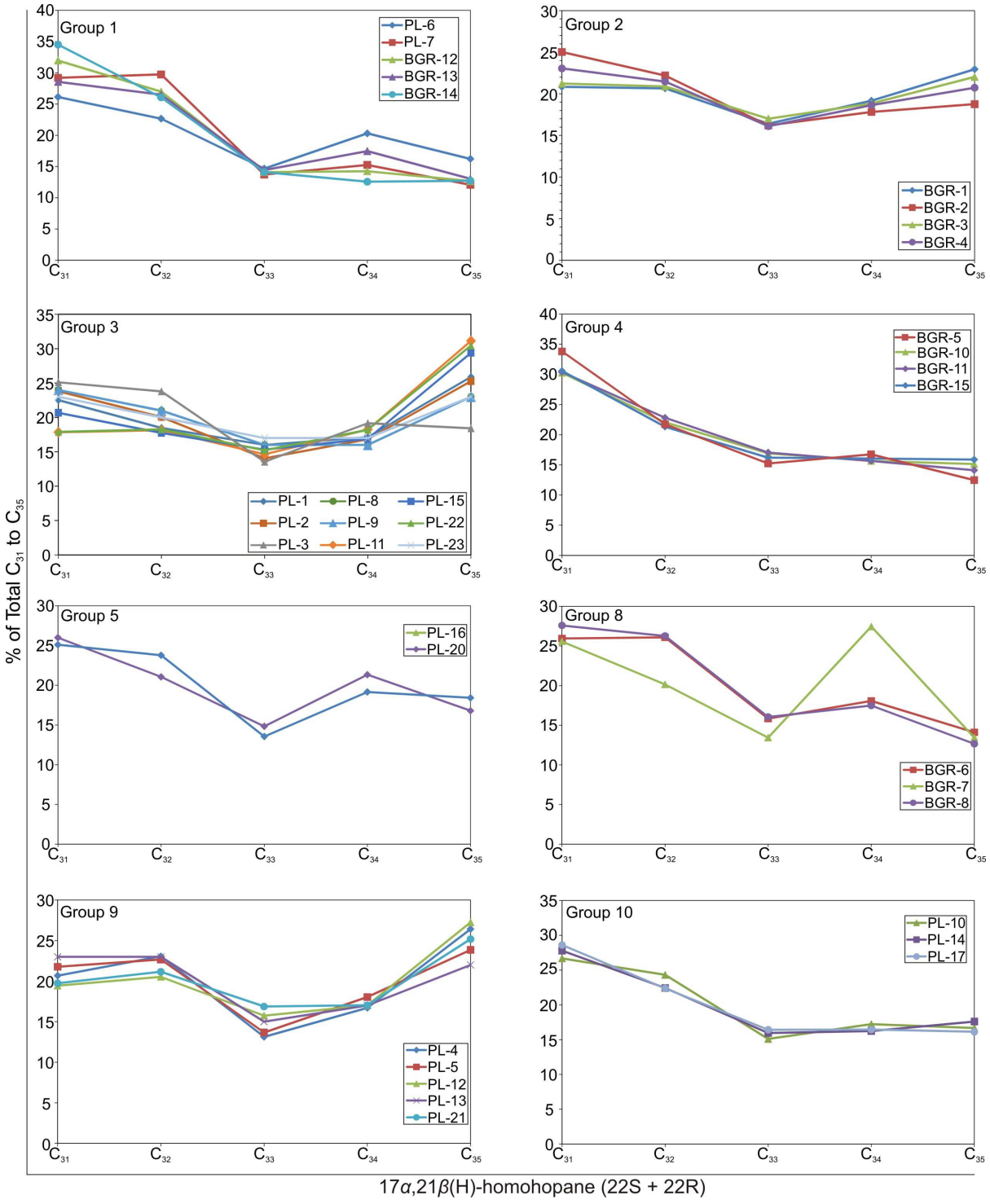

Fig. 7. Homohopane distributions in Ca2 oils. BGR-9, PL-18, -19 and -24 are not plotted because of absent or reduced homohopanes.

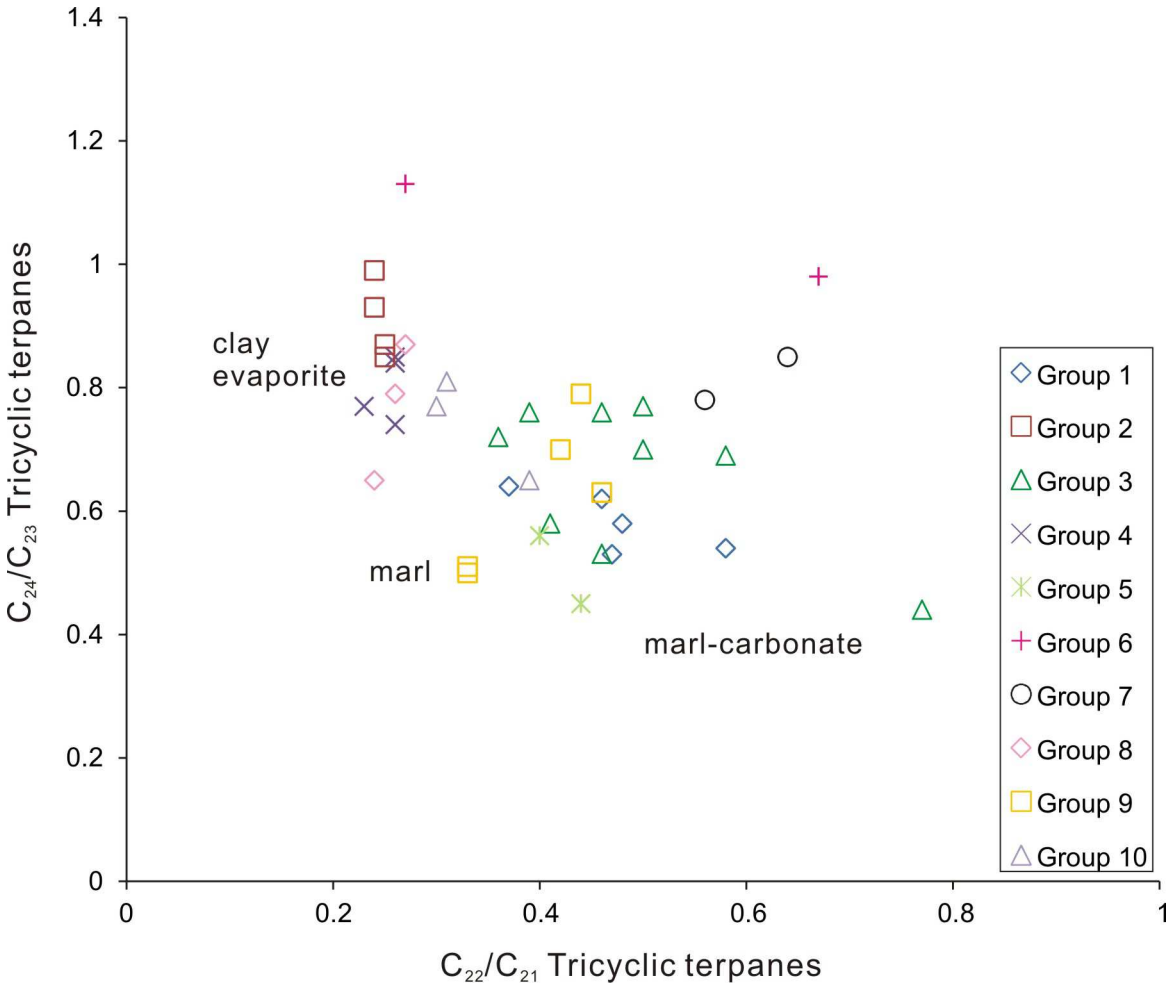

Fig. 8. C_{24}/C_{23} versus C_{22}/C_{21} of tricyclic terpanes for the studied oils used to infer source rock lithology from oil composition (Peters et al., 2005).

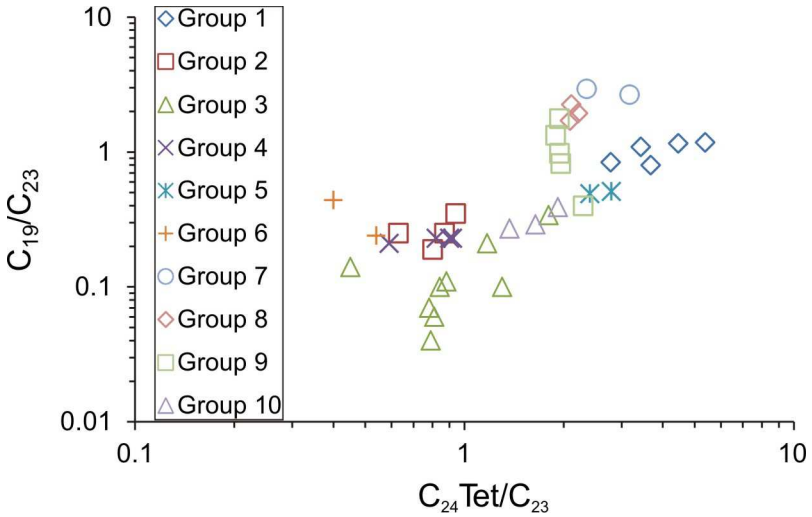

Fig. 9. C_{24} tetracyclic (Tet)/C_{23} tricyclic terpanes versus C_{19}/C_{21} tricyclic terpanes for Ca2 oil samples used to infer source rock lithology from oil composition. Oil groups are differentiated and facies-controlled. High abundance of C_{24} Tet might indicate carbonate-evaporite depositional environment of source rocks for Ca2 oils.

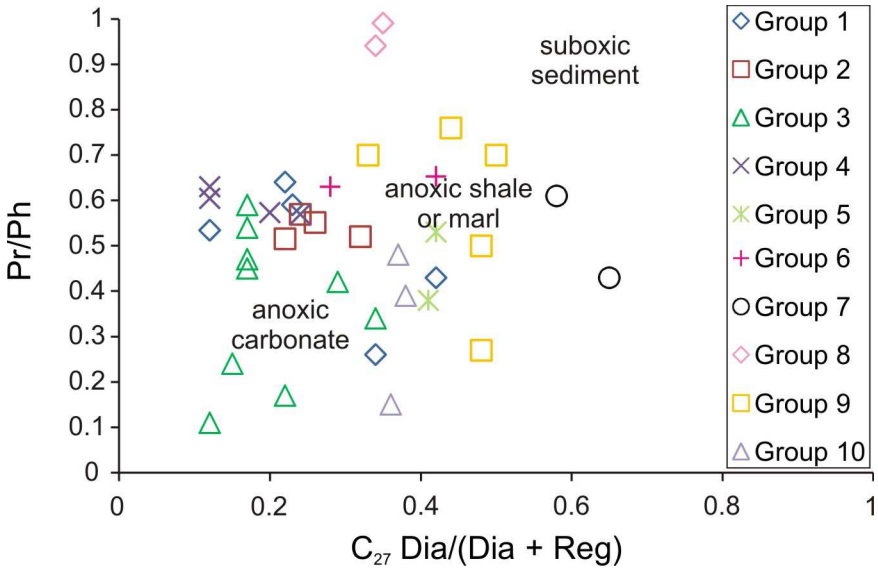

Fig. 10. Correlation between pristane/phytane (Pr/Ph) and C_{27} diasteranes/(diasteranes + regular steranes) obtained from extracts of Ca2 oils showing that the correlation is controlled by the depositional environment of source rocks for Ca2 hydrocarbons (fields modified after Moldowan et al., 1994).

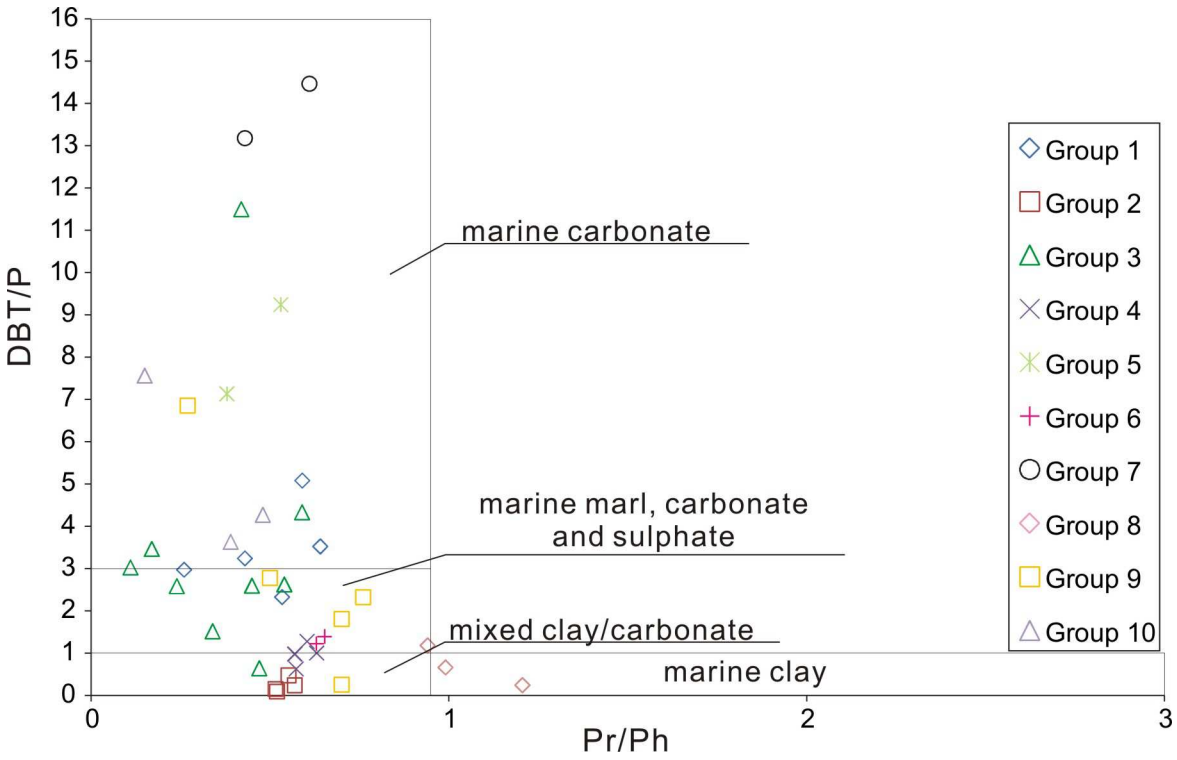

Fig. 11. Cross-plot of dibenzothiophene/phenanthrene (DBT/P) ratio versus pristane/phytane (Pr/Ph) ratio for Ca2 oil samples (graphical fields modified after Hughes et al., 1985).

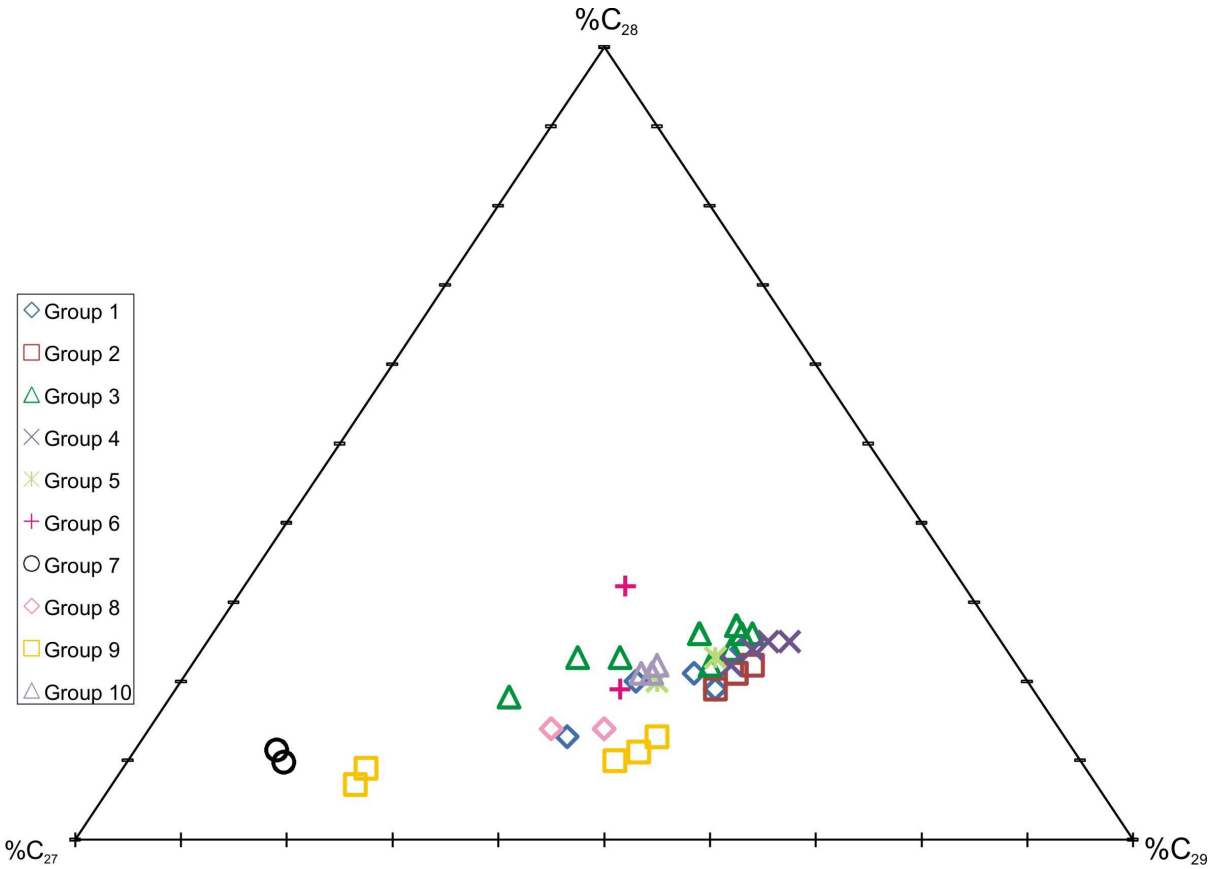

Fig. 12. Ternary diagram of C_{27}-, C_{28}-, and C_{29}ααα (20R)-sterane distributions for the analysed Ca2 oil samples.

Group	Wells	Oil field	Depth (m)	$\delta^{13}C_{SAT}$	$\delta^{13}C_{ARO}$	CV	Pr/Ph	Pr/*n*-C_{17}	Ph/*n*-C_{18}	C_{19}/C_{23}	C_{22}/C_{21}	C_{24}/C_{23}	$C_{24}Tet/C_{23}$	C_{26}/C_{25}
1	BGR-12	Döbern	-	-25.8	-24.9	-1.65	0.53	0.13	0.34	0.84	0.37	0.64	2.78	1.01
1	BGR-13	Guben	-	-25	-24.2	-2.12	0.64	0.08	0.20	1.16	0.58	0.54	4.45	0.92
1	BGR-14	Tauer	-	-26.1	-24.3	0.44	0.59	0.10	0.23	1.09	0.47	0.53	3.43	1
1	PL-6	Kosarzyn	1753.5-1788	-24.3	-23.9	-3.23	0.26	0.07	0.39	0.8	0.48	0.58	3.67	0.89
1	PL-7	Kosarzyn	1810.7-1817.5	-25.7	-24.9	-1.91	0.43	0.11	0.37	1.18	0.46	0.62	5.37	0.81
2	BGR-1	Richtenberg	-	-27	-26.3	-1.73	0.52	0.57	1.11	0.25	0.24	0.93	0.87	0.78
2	BGR-2	Reinkenhagen	-	-26.8	-26.5	-2.68	0.57	0.49	0.93	0.25	0.25	0.87	0.63	0.84
2	BGR-3	Barth	-	-27.1	-26.2	-1.25	0.55	0.48	0.87	0.35	0.24	0.99	0.94	0.84
2	BGR-4	Grimmen	-	-27.5	-25.1	2.2	0.52	0.57	1.16	0.19	0.25	0.85	0.80	0.76
3	PL-1	Błotno	3181.5-3184	-26.8	-26.1	-1.78	0.42	0.37	0.83	0.14	0.39	0.76	0.45	0.91
3	PL-2	Daszewo	2891.8-2910	-27	-26.6	-2.29	0.17	0.09	0.59	0.21	0.77	0.44	1.17	0.85
3	PL-3	Daszewo N	2842.5-2843.3	-26.2	-25.8	-2.64	0.34	0.18	0.69	0.34	0.46	0.53	1.8	1.06
3	PL-8	Kamień Pomorski	2232	-27.3	-25.9	-0.07	0.54	0.49	1	0.04	0.5	0.7	0.79	0.83
3	PL-9	Kamień Pomorski	2246	-27.4	-26	-0.09	0.45	0.44	0.96	0.06	0.5	0.77	0.81	0.84
3	PL-11	Międzyzdroje	2824.5-2836.5	-27.2	-26.5	-1.66	0.11	0.11	1.27	0.1	0.36	0.72	1.3	0.26
3	PL-15	Rekowo	2666-2667	-26.6	-26.1	-2.29	0.59	0.86	0.99	0.1	0.41	0.58	0.84	0.67
3	PL-22	Wapnica	3015-3029	-27.4	-26.5	-1.16	0.24	0.29	1.24	0.11	0.46	0.76	0.88	0.59
3	PL-23	Wysoka Kamieńska	3030	-27.4	-26.2	-0.37	0.47	0.44	0.96	0.07	0.58	0.69	0.78	0.76
4	BGR-5	Fallstein	-	-27.2	-26.2	-1	0.63	0.42	0.74	0.21	0.23	0.77	0.59	0.86
4	BGR-10	Mittweide	-	-26.7	-26.1	-2.04	0.57	0.45	0.88	0.23	0.26	0.85	0.82	0.85
4	BGR-11	Pillgram	-	-27.2	-26.2	-1	0.57	0.47	0.93	0.23	0.26	0.84	0.92	0.83
4	BGR-15	Schlepzig	-	-27.6	-26.1	0.24	0.60	0.42	0.83	0.23	0.26	0.74	0.90	0.88
5	PL-16	Retno	1700-1730	-27.3	-27.1	-2.74	0.53	0.37	0.64	0.49	0.4	0.56	2.4	0.52
5	PL-20	Struga	2042.5-2058.5	-27.6	-27.6	-3.09	0.38	0.17	0.54	0.51	0.44	0.45	2.79	0.62
6	BGR-9	Kietz	-	-26.5	-25.8	-1.88	0.65	0.41	0.71	0.44	0.27	1.13	0.4	1.1
6	PL-24	Namyślin	3140	-26.4	-25.4	-1.25	0.63	0.44	0.71	0.24	0.67	0.98	0.54	1.19
7	PL-18	Sławoborze	3242-3258	-27.9	-27.8	-2.86	0.61	0.19	0.47	2.66	0.56	0.78	3.17	0.54
7	PL-19	Sławoborze	3207-3238	-28.1	-27.9	-2.38	0.43	0.17	0.52	2.94	0.64	0.85	2.35	1.15
8	BGR-6	Volkenroda	-	-28.7	-28.6	-2.53	0.94	0.50	0.63	1.94	0.27	0.87	2.21	1
8	BGR-7	Altengoltern	-	-28.5	-29.2	-4.37	1.21	0.35	0.37	2.25	0.24	0.65	2.11	1.22
8	BGR-8	Mehrstedt	-	-29.2	-28.3	-0.6	0.99	0.56	0.68	1.71	0.26	0.79	2.09	1.07
9	PL-4	Gorzysław	2417-2420.5	-30.6	-30.6	-2.16	0.5	0.78	1.5	0.98	0.33	0.5	1.94	1.19
9	PL-5	Gorzysław	2728-2746	-30.5	-31.0	-3.31	0.7	1.17	1.43	0.82	0.33	0.51	1.96	0.44
9	PL-12	Moracz	3279.5-3309.5	-30.5	-30.1	-1.31	0.27	0.18	0.89	1.33	0.42	0.7	1.89	0.67
9	PL-13	Petrykozy	2623	-30.3	-29.9	-2.26	0.7	0.56	0.91	0.4	0.44	0.79	2.29	0.87
9	PL-21	Wapnica	2812.5-2818.5	-29.9	-29.9	-1.37	0.76	0.57	0.84	1.77	0.46	0.63	1.94	0.72
10	PL-10	Maszewo	1657-1666	-26.3	-26	-2.83	0.15	0.08	0.73	0.39	0.39	0.65	1.92	1.16
10	PL-14	Połęcko	1560.4-1576.9	-26.6	-26	-2.07	0.39	0.33	0.8	0.29	0.3	0.77	1.64	0.71
10	PL-17	Rybaki	1668-1708.5	-25.9	-25.6	-2.95	0.48	0.45	0.8	0.27	0.31	0.81	1.37	0.5

1048

1049

BNH/H	C_{29}/H	C_{30} dia/H	C_{31}R/H	G/C_{30}	HHI	C_{32}/C_{31} (S+R)	C_{34}/C_{33} (S+R)	C_{35}S/C_{34}S	%C_{31}	%C_{32}	%C_{33}	%C_{34}	%C_{35}
0	0.65	0.05	0.38	0.14	0.13	0.84	1.01	0.89	32	27	14	14	13
0	0.67	0.04	0.43	0.15	0.13	0.93	1.21	0.74	29	27	14	17	13
0	0.8	0.05	0.42	0.15	0.13	0.76	0.89	1.02	35	26	14	13	13
0.07	0.48	0.08	0.54	0.24	0.16	0.87	1.38	0.76	26	23	15	20	16
0.07	0.66	0.11	0.64	0.21	0.12	1.02	1.11	0.77	29	30	14	15	12
0	0.39	0.03	0.39	0.19	0.23	0.99	1.17	1.19	21	21	16	19	23
0	0.42	0.03	0.38	0.16	0.19	0.89	1.10	1.04	25	22	16	18	19
0	0.37	0.03	0.38	0.18	0.22	0.98	1.11	1.17	21	21	17	19	22
0	0.39	0.03	0.37	0.16	0.21	0.93	1.16	1.11	23	21	16	19	21
0.03	0.68	0.07	0.46	0.35	0.26	0.82	1.07	1.56	23	18	16	17	26
0.03	0.94	0.04	0.48	0.21	0.25	0.84	1.2	1.47	24	20	14	17	25
0	0.65	0.06	0.48	0.14	0.18	0.95	1.41	0.94	25	24	14	19	18
0.01	0.62	0.02	0.36	0.17	0.21	0.87	0.72	1.38	24	21	16	16	23
0.01	0.63	0.02	0.36	0.18	0.24	0.86	0.72	1.37	24	21	16	16	23
0.01	0.59	0.01	0.41	0.25	0.31	1.02	1.25	1.7	18	18	15	18	31
0.03	0.65	0.03	0.44	0.23	0.29	0.86	1.1	1.71	21	18	15	17	29
0.02	0.56	0.03	0.39	0.24	0.3	1.02	1.2	1.65	18	18	15	18	30
0.01	0.57	0.03	0.37	0.2	0.26	0.88	0.72	1.4	23	20	17	17	23
0	0.56	0.03	0.4	0.13	0.12	0.64	1.10	0.74	34	22	15	17	12
0	0.5	0.03	0.42	0.13	0.15	0.73	0.93	0.96	30	22	17	16	15
0	0.49	0.03	0.41	0.10	0.14	0.75	0.92	0.92	30	23	17	16	14
0	0.57	0.04	0.39	0.12	0.16	0.70	0.99	0.99	31	21	16	16	16
0.06	0.54	0.07	0.5	0.23	0.17	0.87	1.22	0.89	27	23	15	18	17
0.06	0.71	0.07	0.51	0.27	0.17	0.81	1.44	0.75	26	21	15	21	17
0	2.03	0	0	0.00	0	0.00	0.00	0	0	0	0	0	0
0.06	0.84	0.2	0.15	0.20	0	0.55	0	0	54	30	16	0	0
0.21	5.78	0	1.67	0	0	0	0	0	100	0	0	0	0
0.18	4.36	0	1.1	0	0	0	0	0	100	0	0	0	0
0	0.41	0.03	0.37	0.19	0.14	1.01	1.14	0.77	26	26	16	18	14
0	0.68	0.04	0.42	0.20	0.13	0.79	2.04	0.39	26	20	13	27	13
0	0.43	0.03	0.34	0.20	0.13	0.95	1.09	0.70	28	26	16	17	13
0.05	0.57	0.16	0.56	0.41	0.26	1.12	1.27	1.48	21	23	13	17	26
0.04	0.31	0.08	0.56	0.35	0.24	1.04	1.32	1.28	22	23	14	18	24
0.01	0.4	0.28	0.36	0.19	0.27	1.06	1.08	1.59	19	21	16	17	27
0.02	0.4	0.18	0.34	0.11	0.27	1	0.78	1.31	23	23	15	17	22
0.03	0.38	0.29	0.34	0.2	0.25	1.07	1.01	1.43	20	21	17	17	25
0.03	0.51	0.07	0.51	0.23	0.17	0.91	1.14	0.94	27	24	15	17	17
0.02	0.49	0.06	0.58	0.22	0.18	0.81	1.02	1.05	28	22	16	16	18
0.05	0.39	0.06	0.53	0.2	0.16	0.78	1	0.97	29	22	16	16	16

C_{29} dia/(dia+reg)	C_{27}dia/(dia+reg)	$\%C_{27}$	$\%C_{28}$	$\%C_{29}$	C_{27}/C_{29}	C_{28}/C_{29}	tricyclics/17α-hopanes	steranes/17α-hopanes	ISO	CHL	DBT/P	CPI
0.22	0.12	25	24	51	0.49	0.46	0.16	0.52	45	12	2.32	0.93
0.31	0.22	31	19	51	0.61	0.37	0.15	0.17	nd	nd	3.52	0.94
0.32	0.23	31	21	48	0.65	0.44	0.30	0.26	49	nd	5.08	0.99
0.15	0.34	37	20	43	0.7	0.47	0.06	0.18	60	4	2.97	0.93
0.32	0.42	47	13	40	0.91	0.48	0.03	0.1	16	1	3.24	0.91
0.32	0.32	30	19	51	0.59	0.36	0.10	0.79	408	65	0.09	0.88
0.24	0.24	27	21	52	0.53	0.39	0.16	0.91	163	27	0.24	0.91
0.28	0.26	27	21	52	0.51	0.41	0.15	1.01	159	27	0.47	0.92
0.24	0.22	25	22	53	0.48	0.42	0.10	0.92	360	47	0.15	0.89
0.14	0.29	37	23	40	0.69	0.51	0.15	0.28	161	9	11.5	0.99
0.11	0.22	41	23	36	0.87	0.54	0.09	0.17	73	4	3.46	0.93
0.27	0.34	50	18	32	0.98	0.51	0.05	0.12	23	nd	1.5	0.92
0.17	0.17	24	26	50	0.48	0.52	0.11	0.34	275	44	2.62	0.96
0.17	0.17	23	26	51	0.45	0.51	0.11	0.32	22	3	2.59	0.98
0.04	0.12	26	24	50	0.47	0.57	0.05	0.35	585	26	3.02	0.94
0.05	0.17	28	26	46	0.52	0.41	0.06	0.29	320	19	4.33	0.93
0.05	0.15	29	22	49	0.51	0.32	0.06	0.35	710	26	2.58	0.94
0.21	0.17	24	27	49	0.49	0.55	0.11	0.32	117	53	0.64	0.97
0.2	0.12	20	25	55	0.36	0.45	0.50	2.04	58	21	1.00	0.97
0.24	0.20	24	24	52	0.46	0.46	0.32	1.15	125	19	0.62	0.91
0.27	0.24	27	22	51	0.52	0.43	0.18	0.71	230	27	0.98	0.91
0.18	0.12	22	25	53	0.41	0.47	0.26	1.37	145	17	1.27	0.96
0.17	0.42	28	23	49	0.53	0.53	0.05	0.17	50	nd	9.24	0.91
0.20	0.41	35	20	45	0.66	0.48	0.05	0.12	46	4	7.13	0.92
0.49	0.42	39	19	42	0.93	0.46	5.32	1.83	nd	nd	1.39	0.98
1.98	0.28	32	32	36	0.89	0.89	0.53	0.65	nd	nd	1.22	0.99
2.99	0.58	75	11	13	4.45	1.36	0.53	1.07	nd	nd	14.47	0.95
3.02	0.65	75	10	15	3.55	1.42	0.49	0.75	nd	nd	13.18	0.94
0.54	0.34	43	14	43	0.98	0.33	0.27	0.52	nd	nd	1.18	0.95
0.62	0.32	47	14	38	1.23	0.37	1.47	1.04	nd	nd	0.24	0.98
0.54	0.35	43	14	43	1.01	0.32	0.23	0.43	nd	nd	0.65	0.96
0.29	0.48	39	13	49	0.44	0.38	0.04	0.31	nd	nd	2.78	0.85
0.33	0.5	41	11	48	0.58	0.4	0.04	0.27	nd	nd	1.81	0.88
0.78	0.48	68	9	23	1.68	0.86	0.14	0.37	nd	nd	6.85	0.95
0.47	0.33	44	10	46	0.33	0.31	0.1	0.2	nd	nd	0.25	0.92
0.76	0.44	70	7	23	1.72	0.83	0.15	0.36	nd	nd	2.32	0.94
0.18	0.36	36	21	43	0.64	0.48	0.06	0.23	141	6	7.56	0.93
0.15	0.38	34	22	44	0.62	0.52	0.06	0.28	234	6	3.63	0.93
0.16	0.37	35	21	44	0.64	0.48	0.07	0.32	341	14	4.27	0.93

Table 1. Source-related geochemical characteristics of Ca2 oil samples.

nd – not determined;

$\delta^{13}C_{SAT}$ – stable carbon isotopic composition (‰) of the saturated hydrocarbon fraction;

$\delta^{13}C_{ARO}$ – stable carbon isotopic composition (‰) of the aromatic hydrocarbon fraction;

CV – canonical variable ($CV = -2.53\delta^{13}C_{SAT} + 2.22\delta^{13}C_{ARO} - 11.65$);

Pr/Ph – pristane/phytane;

Pr/*n*-C_{17} – pristane/*n*-heptadecane;

Ph/*n*-C_{18} – phytane/*n*-octadecane;

C_{19}/C_{23} – C_{19}/C_{23} tricyclic terpanes;

C_{22}/C_{21} – C_{22}/C_{21} tricyclic terpanes;

C_{24}/C_{23} – C_{24}/C_{23} tricyclic terpanes;

C_{24}Tet/C_{23} – C_{24} tetracyclic/C_{23} tricyclic terpanes;

C_{26}/C_{25} – C_{26}/C_{25} tricyclic terpanes;

BNH/H – 28,30-bisnorhopane / C_{30} 17α-hopane;

C_{29}/H – C_{29} norhopane / C_{30} 17α-hopane;

C_{30} dia/H – C_{30} diahopane / C_{30} 17α-hopane;

C_{31}R/H – C_{31} homohopane 22R / C_{30} 17α-hopane;

G/H – gammacerane / C_{30} 17α-hopane;

HHI – homohopane index: $C_{35}\alpha\beta$(S + R) / (ΣC_{31}-$C_{35}\alpha\beta$ S + R);

C_{32}/C_{31} (S+R) – C_{32} (S+R) 17α-hopane / C_{31} (S+R) 17α-hopane;

C_{34}/C_{33} (S+R) – C_{34} (S+R) 17α-hopane / C_{33} (S+R) 17α-hopane;

$C_{35}S/C_{34}S$ – $C_{35}S/C_{34}S$ homohopanes;

%C_{31}, %C_{32}, %C_{33}, %C_{34}, %C_{35} – percentage of C_{31}, C_{32}, C_{33}, C_{34}, C_{35} to total $C_{31\text{-}35}$ homohopanes;

C_{29} dia – diasterane/sterane ratio – C_{29} 13β,17α(H) (20S + 20R) / (C_{29} 5α,14α,17α(H) 20S + 20R + 5α,14β,17β(H) 20S + 20R);

%C_{27} (*m*/*z* 217) – 100 x $C_{27}S$ / ($C_{27}S$ + $C_{28}S$ + $C_{29}S$);

%C_{28} (*m*/*z* 217) – 100 x $C_{28}S$ / ($C_{27}S$ + $C_{28}S$ + $C_{29}S$);

%C_{29} (*m*/*z* 217) – 100 x $C_{29}S$ / ($C_{27}S$ + $C_{28}S$ + $C_{29}S$);

C_{27}/C_{29} – C_{27}/C_{29} sterane ratio;

C_{28}/C_{29} - C_{28}/C_{29} sterane ratio;

tricyclics/17α-hopanes – $\Sigma C_{19\text{-}26}$ tricylic terpanes / ($\Sigma C_{19\text{-}26}$ tricylic terpanes + $\Sigma C_{29\text{-}33}$ 17α-hopanes);

steranes/17α-hopanes – $\Sigma C_{27\text{-}29}$ regular steranes / $\Sigma C_{28\text{-}35}$ 17α-hopanes;

ISO – isorenieratane (µg/g oil);

CHL – chlorobactane (µg/g oil);

DBT/P – dibenzothiophene/phenanthrene;

CPI – carbon preference index based on *n*-alkanes [$\Sigma(C_{25}–C_{33})_{odd}$ / $\Sigma(C_{24}–C_{32})_{even}$ + $\Sigma(C_{25}–C_{33})_{odd}$ / $\Sigma(C_{26}–C_{34})_{even}$] / 2

Group	Wells	C_{27} Ts/Tm	M/H	C_{29} 20S	C_{29} ββ	TA(I)/TA(I+II)	MDR	Rm
1	BGR-12	1.14	0.12	0.51	0.57	0.23	2.98	0.73
1	BGR-13	1.36	0.14	0.45	0.55	0.25	2.52	0.69
1	BGR-14	2.44	0.18	0.49	0.55	0.55	3.32	0.75
1	PL-6	1.43	0.1	0.47	0.58	0.26	2.10	0.72
1	PL-7	1.11	0.13	0.43	0.56	0.16	1.96	0.71

2	BGR-1	0.87	0.10	0.50	0.54	0.05	5.89	0.94
2	BGR-2	0.95	0.09	0.48	0.53	0.06	3.24	0.75
2	BGR-3	1.3	0.07	0.49	0.58	0.12	2.51	0.69
2	BGR-4	0.73	0.10	0.50	0.54	0.04	4.04	0.80
3	PL-1	3.5	0.06	0.51	0.57	0.30	2.18	0.72
3	PL-2	1.1	0.09	0.5	0.59	0.22	2.65	0.74
3	PL-8	0.92	0.05	0.54	0.53	0.14	1.58	0.63
3	PL-9	0.91	0.06	0.56	0.52	0.12	2.04	0.66
3	PL-11	0.63	0.06	0.47	0.56	0.1	1.76	0.70
3	PL-15	0.98	0.07	0.48	0.56	0.08	1.78	0.70
3	PL-22	0.77	0.08	0.48	0.57	0.11	1.76	0.70
3	PL-23	1.23	0.1	0.55	0.57	0.09	3.30	0.75
4	BGR-5	1.13	0.09	0.49	0.58	0.11	3.90	0.79
4	BGR-10	1.26	0.12	0.51	0.58	0.24	3.63	0.78
4	BGR-11	0.9	0.10	0.50	0.58	0.32	2.51	0.69
4	BGR-15	0.79	0.10	0.51	0.59	0.16	3.55	0.77
5	PL-3	0.77	0.11	0.53	0.58	0.2	2.16	0.72
5	PL-16	1.85	0.1	0.46	0.58	0.21	1.76	0.70
5	PL-20	1.42	0.1	0.47	0.56	0.24	2.05	0.71
6	BGR-9	5.23	nd	0.50	0.59	0.83	3.76	0.78
6	PL-24	2.13	nd	nd	nd	nd	2.98	0.73
7	PL-18	11.77	nd	nd	0.55	1.00	4.91	0.91
7	PL-19	10.9	nd	nd	0.57	1.00	4.53	0.85
8	BGR-6	0.81	0.08	0.51	0.59	0.41	5.54	0.91
8	BGR-7	0.94	0.17	0.50	0.57	1	8.31	1.12
8	BGR-8	1.32	0.09	0.50	0.59	0.39	5.64	0.92
9	PL-4	0.76	0.19	0.49	0.57	0.10	1.59	0.68
9	PL-5	0.83	0.09	0.48	0.55	0.08	1.48	0.67
9	PL-12	4.01	0.15	0.5	0.61	0.38	2.59	0.74
9	PL-13	1.95	0.08	0.56	0.52	0.19	1.80	0.64
9	PL-21	2.99	0.16	0.51	0.62	0.36	3.77	0.78
10	PL-10	1.55	0.12	0.48	0.56	0.19	1.72	0.69
10	PL-14	1.17	0.11	0.47	0.55	0.12	1.63	0.69
10	PL-17	1.4	0.1	0.44	0.54	0.13	1.82	0.70

Table 2. Selected biomarker maturity and maturity-controlled parameters for Ca2 oil samples.

nd – not determined;

C_{27} Ts/Tm – C_{27} 18α-trisnorneohopane / 17α-trisnorhopane;

M/H – moretane/hopane;

C_{29} 20S – 20S / (20S + 20R) epimers of 5α(H),14α(H),17αβ(H)-ethylsterane;

C_{29} ββ – 5α(H),14β(H),17β(H)/[5α(H),14β(H),17β(H) + 5α(H),14α(H),17α(H) 20R ethylsteranes];

TA(I)/TA(I+II) – TA(I) = C_{20}+C_{21}, TA(II) = ΣC_{26}-C_{28} (20S + 20R) triaromatic steroids;

MDR – methyldibenzothiophene ratio = 4-MDBT / 1-MDBT;

R_m – calculated vitrinite reflectance = 0.073 x MDR + 0.51